Accepted Manuscript

Research papers

Numerical modeling of a regional groundwater flow system to assess groundwater storage loss, capture and sustainable exploitation of the transboundary Milk River Aquifer (Canada – USA)

Marie-Amélie Pétré, Alfonso Rivera, René Lefebvre

PII: S0022-1694(19)30503-7
DOI: https://doi.org/10.1016/j.jhydrol.2019.05.057
Reference: HYDROL 23790

To appear in: *Journal of Hydrology*

Received Date: 20 February 2019
Revised Date: 15 May 2019
Accepted Date: 19 May 2019

Numerical modeling of a regional groundwater flow system to assess groundwater storage loss, capture and sustainable exploitation of the transboundary Milk River Aquifer (Canada – USA)

Marie-Amélie Pétré[ab], Alfonso Rivera[a], René Lefebvre[b]

[a]Geological Survey of Canada, Québec Division, Québec, QC, Canada

[b]Institut national de la recherche scientifique, Centre Eau Terre Environnement, Québec, QC, Canada

Corresponding author : Marie-Amélie Pétré

Present adress : Laboratoire HydroSciences Montpellier UMR 5569 UM, CNRS, IRD

ABSTRACT

Groundwater capture and storage loss play a major role in the sustainable exploitation of a regional aquifer. This study aimed to identify the impact of major and long-term groundwater exploitation on a regional aquifer system to understand the processes controlling the sustainable exploitation of the transboundary Milk River Aquifer (MRA). The MRA extends over 26,300 km^2, being a major water resource across southern Alberta (Canada) and northern Montana (USA). Concerns about the sustainability of the MRA were raised as the century-old exploitation has led to important drawdowns and the local loss of historical artesian conditions. A steady-state numerical model of the regional flow system was developed and calibrated against hydraulic heads, groundwater fluxes, and the area with flowing artesian wells. Four groundwater abstraction scenarios were simulated: 1) natural flow conditions without exploitation; 2) the mean abstraction rate over the last 108 years; 3) the historical maximum global abstraction rate of the

MRA; and 4) a theoretical high abstraction rate based on the maximum rate estimated for each MRA exploitation zone. The numerical model agrees with the previously formulated conceptual model and supports its hydraulic plausibility. Results show that MRA exploitation has led to a major change in flow patterns to sustain groundwater abstraction. The MRA water balance under exploitation indicates that more recharge and reduced seepage to bedrock valleys compensate groundwater withdrawals. Based on its impact on regional discharge and the reduction in MRA storage, the mean historical level of exploitation of the MRA appears sustainable. Larger exploitation rates would significantly reduce groundwater discharge to surface seepage locations and lead to a larger reduction in groundwater storage in the MRA. Modeling also illustrates that the MRA is an internationally shared resource. This situation would justify a joint management of the aquifer system between Canada and USA; especially in the area comprised between the recharge area in Montana and the Canadian reach of the Milk River.

Keywords: Regional aquifer, Sustainable exploitation, Numerical modelling, Storage changes, Capture, Transboundary aquifer

1. Introduction

Numerical groundwater flow models have proven to be efficient tools to address a variety of water related issues. Applications includes the assessment of sustainable groundwater exploitation, transport of groundwater contaminants, the determination or control of saltwater intrusion (Alwathaf and Mansouri, 2012; Bordeleau et al., 2008; Gaur et al., 2011; Giambastiani et al., 2007; Islam et al., 2016; Meyer, 2014; Sowe, 2017).

At the basin scale, numerical models can provide a better understanding of regional groundwater flow systems, including cross-formational flow through the aquitards, following the pioneering work of Toth (1963) and Freeze and Witherspoon (1966a, 1966b). Numerous numerical modelling studies have provided examples of regional groundwater flow (Janos et al., 2018; Lavigne et al., 2010; Michael and Voss, 2009; Rabelo and Wendland, 2009; Voss and Soliman, 2014; Zhou and Li, 2011). To assess the conditions required for the sustainable exploitation of a regional aquifer, it is necessary to determine the impact of exploitation on the flow system, which is controlled in part by the hydraulic connections between the hydrogeological units and surface water features composing the regional flow system. As initially stated by Theis (1940) and more recently by Konikow and Leake (2014), during groundwater withdrawal part of the groundwater is derived from storage, but over time the aquifer system adjusts to pumping through an increase in recharge or a decrease in discharge, which is called capture. Groundwater capture and storage loss are key concepts related to the sustainability of aquifer exploitation (Konikow, 2015; Konikow and Leake, 2014) and should be quantified while investigating the sustainable exploitation of a regional aquifer system.

In that perspective, the objective of the present study is to develop a numerical model to assess the regional groundwater flow dynamics of a major aquifer under both natural and exploitation conditions to determine the conditions required for the sustainable management of groundwater resources. More specifically, the role of groundwater capture and storage loss will be evaluated at the regional scale.

The transboundary Milk River Aquifer (MRA) constitutes a perfect example of a regional aquifer comprised in a large groundwater flow system. It is also part of a worldwide inventory of transboundary aquifers whose characterization and management are the objects of recent international initiatives such as ISARM or TWAP (IGRAC, 2015; Rivera and Candela, 2018; TWAP, 2012). The MRA extends 26,300 km^2 over southern Alberta (Canada) and northern

Montana (USA) in a semi-arid region where water shortages are an important issue (Government of Alberta, Alberta water for life, 2006). Concerns have been voiced for many decades about the sustainability and mismanagement of groundwater exploitation from the MRA, with indications of locally significant drawdowns (up to 30 m) and the loss of artesian conditions in some areas (AGRA Earth and Environmental Limited, 1998; Borneuf, 1976; Meyboom, 1960). A steady-state numerical model of the regional groundwater flow system comprising the MRA was developed with the objective of understanding the impact of major and long-term exploitation on the entire aquifer system and to identify the processes controlling the sustainable exploitation of the MRA. The numerical model was based on a previously developed 3D geological model (Pétré et al., 2015) and a hydrogeological conceptual model (Pétré et al., 2016) of the aquifer system integrating the MRA.

A simulation of conditions without groundwater exploitation and three scenarios of groundwater extraction in the MRA are simulated to assess the impact of the MRA exploitation. This model must first verify the plausibility of the previously formulated conceptual model and then determine whether the regional flow system can adjust to the MRA exploitation so that a new sustainable flow pattern is established. Knowing that direct recharge to the MRA does not compensate groundwater abstraction (Pétré et al., 2016), this study also involves the determination of groundwater capture and long-term storage loss.

This paper presents first the study area and the conceptual hydrogeological model of the MRA. The Materials and Methods section describes the numerical model design, calibration criteria and the groundwater use evaluation. Then, the simulation and water budget results are presented, followed by a discussion covering the limitations of the model and the implications for groundwater management.

2. Study area and conceptual hydrogeological model

2.1 Study area

The MRA is located in a semi-arid region, spanning southern Alberta and northern Montana (Fig. 1). The mean annual precipitation is between 250 and 450 mm/y and the potential evapotranspiration ranges from 550 to 578 mm/y (Climate Canada, 2015; NOAA, 2015). The topographic highs in the region are the Sweet Grass Hills and Bears Paw Mountains in Montana, and the Cypress Hills and Milk River Ridge in Alberta. The Sweetgrass Hills are an ensemble of three buttes south of the international border. The hydrography of the region includes the transboundary Milk River, the shallow Pakowki Lake and several valleys with intermittent streams called “coulees” (e.g., Etzikom, Chin and Forty Mile coulees).

The stratigraphic sequence in the study area, from the base to the surface, is as follows: the 500-m thick regional aquitard of the Colorado Group underlies the study area. The shales of the Colorado Group contain several thin sandstone beds, the most significant being the 25-m thick Bow Island Sandstone. The Colorado Group is overlain by the Milk River Formation (called Eagle Formation in Montana), which is subdivided into three members in Alberta: the basal Telegraph Creek Member, the middle Virgelle Member and the upper Deadhorse Coulee Member. The Virgelle Member constitutes the MRA as it is the most important aquifer unit within the Milk River Formation. The Milk River Formation (about 100 m thick) subcrops or outcrops near the international border in Alberta, in rings around the Sweetgrass Hills and also following two branches on both sides of the Sweetgrass Arch (the outcrop area is shown on Fig. 1). The Milk River Formation is overlain by the low-permeabilty shales of the Pakowki/Claggett Formation (about 130 m thick). The Belly River Group (Judith River Formation in Montana) overlies the Pakowki/Claggett aquitard and is also considered as an aquifer. With the exception of the topographic highs and coulees, the study area is covered by glacial drift which consists mainly of low-permeability till, typically less than 2 m in thickness (Hendry and Buckland, 1990).

Buried valleys (bedrock channels) are present across the study area (Fig. 1). These buried valleys are preglacial stream valleys buried under glacial drift (Cummings et al., 2012a). In southern Alberta, the Medicine Hat, Skiff and Foremost buried valleys are up to 10 km wide and are incised up to 30 m into bedrock (HCL consultants, 2004; Hendry and Buckland, 1990). Buried valleys locally constitute productive aquifers where the fill material is predominantly sand and gravel (Cummings et al., 2012a; Farvolden et al., 1963; HCL consultants, 2004).

The extent of the numerical model described in this paper follows the hydrogeological limits of the MRA previously defined by Pétré et al. (2016) in the west, north and east (Fig. 1). The north-eastern hydrogeological limit of the MRA corresponds to a low permeability facies hosting the Medicine Hat natural gas fields. In the south, the Marias River and Cut Bank Creek have been chosen as the physiographic limits of the model, although the MRA may extend farther south in Montana. In the south-east corner, the numerical model is limited by the extent of the geological model developed by Pétré et al. (2015) (at longitude -110º), which is the basis of the numerical model.

2.2 Conceptual hydrogeological model

The conceptual hydrogeological model of the MRA developed by Pétré et al., (2016) was used as a basis for the development of the numerical groundwater flow model. Only a brief description of the conceptual model is presented here since details can be found in Pétré et al. (2016). Figure 2 shows a cross-section through the MRA from its outcrop area at high elevation to its downgradient limit (location of line AA' shown on Fig. 1). The MRA is a typical confined aquifer, radially dipping from the outcrop/subcrop areas (Fig. 2). Direct recharge of the MRA occurs mainly in the outcrop or subcrop areas of the Milk River Formation where unconfined conditions and modern groundwaters are present, as indicated by the presence of tritium (Pétré et al., 2016). Groundwater inflow into the MRA also occurs through subsurface vertical inflow from overlying geological units in the topographic highs of the study area. Groundwater flow diverges from the Sweetgrass Hills to the north, east and southeast. West of the Sweet Grass Arch, groundwater flows south-west and north from a groundwater divide located north of Cut Bank. Two transboundary flowpaths were defined on the basis of a potentiometric map (Pétré et al., 2016): (1) an eastern flowpath from the Sweet Grass Hills to the north and (2) a western flow path from the northern part of Cut Bank to the north.

An abrupt change in the horizontal hydraulic head gradient indicates that the Milk River and part of the Verdigris Coulee intercept a large proportion of the groundwater flowing to the north from direct MRA recharge areas. As no other natural surface discharge feature has been identified, vertical leakage trough the confining units was inferred to be another important natural discharge mechanism. Cross formational flow is enhanced along the talwegs of buried valleys which are acting as drains, as inferred by Toth and Corbet (1986) and shown by Pétré et al. (2016). Indeed, the buried valleys have eroded the upper bedrock (Belly River /Judith River and Pakowki/Claggett formations), thus reducing the thickness of the bedrock between the MRA and surficial sediments. Under the confined conditions found north of the Milk River, the MRA contains a fossil groundwater, not significantly renewed by modern recharge. This fossil signature is demonstrated by the absence of radiocarbon and a $^{36}Cl/Cl$ ratio indicating a groundwater residence time reaching 2 My further north of the MRA (Pétré et al., 2016).

3. Model simulation and calibration

3.1 Model design and boundary conditions

The basis of the numerical groundwater flow model of the aquifer system encompassing the MRA is the three-dimensional (3D) geological model that was previously developed with the software Leapfrog Hydro (Pétré et al., 2015). This software was then used to convert the geological model in a finite element grid compatible with the numerical groundwater flow simulator FEFLOW (Diersch, 2014). A 2D areal finite element mesh was first created in FEFLOW and was then applied to the layers of the 3D geological model, resulting in a 3D numerical model grid comprising 15 layers (Fig. 3). The geometry and thicknesses of the geological layers remained unchanged in the numerical model.

The numerical model covers a surface area of 26,300 km^2 with a volume of approximatively 30,000 km^3. The top surface of the groundwater flow model corresponds to ground level, represented by the Digital Elevation Model (DEM) of the study area (pixel size is 500 m x 500 m). The domain is discretized into 329,825 triangular prismatic mesh elements and 165,587 nodes per slice. The finite element mesh was locally refined along the Milk River where a steep horizontal hydraulic gradient was expected. The lateral sizes of the elements in the mesh vary from 100 m, where the grid was refined, to 650 m in the remainder of the domain.

The model considers seven hydrostratigraphic units (Fig. 3): surficial sediments, bedrock valleys, the Belly/Judith River Formation, the Pakowki/Claggett Formation, the Milk River Formation, the Colorado Group and the Bow Island Sandstone.

Boundary conditions in the model domain are summarized in Fig. 4d.

Specified heads with a seepage constraint were assigned to the streams to precludes any inflow into the model from the stream nodes in accordance with the conceptual model showing losing streams.

A hydraulic head corresponding to ground elevation was assigned to the nodes along the streams (Fig. 4a). The basal layer of the model was defined as a no flow boundary. Along the outer boundary of the domain on layer 14 (corresponding to the Bow Island Sandstone), a specified head boundary condition was set to 750 m. This value is based on the potentiometric map of the Bow Island Sandstone produced by Swanick (1982) in Alberta (Fig. 4b). The recharge rate was set to 0 mm/y where the Colorado Group aquitard outcrops; since this aquitard underlies the MRA, the MRA is absent in these areas. In the outcrop/subcrop area, which constitutes the direct recharge area of the MRA, the recharge rate was set to 10 mm/y, based on previous estimates (Pétré et al., 2016). Elsewhere, the recharge rate was adjusted to 1 mm/y during model calibration (Fig. 4c).

3.2 Hydraulic conductivity of the hydrostratigraphic units

The K value of the MRA was calculated on the basis of the transmissivity and thickness maps of the Milk River Formation derived from the geological model (Pétré et al., 2016, 2015). The K values assigned to the MRA range from 8.1×10^{-9} m/s to 9.4×10^{-4} m/s. The spatial distribution of K (ESM1) was applied to the elements corresponding to the Milk River Formation. Hydraulic conductivity (K) of the hydrostratigraphic units are summarized in Table 2. Except for the MRA, all hydrostratigraphic units were assigned a uniform value based on the limited number of points estimates available. K estimates for most of units were adjusted during calibration given the large uncertainties related to their spatial variability (Table 2).

3.3 Groundwater use evaluation in southern Alberta

Information about groundwater use is limited in the study area because the water right holders do not have the statutory requirement to measure their groundwater withdrawals. An assessment of the historical groundwater use in the MRA for the period 1908-2015 was carried out in southern Alberta by Pétré (2016) using 1655 available wells. An extraction rate was assigned to each well according to their intended use (domestic, stock, municipal or industrial use). For this assessment, six exploitation zones were delineated (Fig. 5) on the basis of the well density and the periods at which these wells were installed in the MRA. Those exploitation zones are represented in the numerical model as diffusive sinks, but the flow rate of the eight main municipal wells were considered as local sinks. To model the impact of MRA, the model was first run without pumping in the MRA to establish natural conditions and then three MRA exploitation scenarios based on the estimated historical exploitation were simulated from the natural conditions scenario (Table 1):

- Scenario 1, mean exploitation rate: this scenario uses the mean exploitation rate in each zone over the 108 years considered, which also corresponds to the overall mean historical exploitation rate of the MRA;
- Scenario 2, maximum exploitation rate: over the years, the exploitation rate of the MRA had steadily increased from 1908 to the mid-1990's and has been in decline since then (Pétré 2016). Thus, this scenario considers the maximum exploitation rate of the mid-1990's, which is spatially distributed over the exploitation zones based on the mean contribution of each zone over the exploitation period;

- Scenario 3, ultimate exploitation rate: MRA exploitation was not uniformly distributed among the exploitation zones, which have had maximum exploitation rates over different periods. This last scenario thus considers an exploitation rate of the MRA that corresponds to the maximum exploitation rate historically reached within each exploitation zone. The overall exploitation rate of the MRA for this scenario is thus larger than the historically reached maximum rate (scenario 2).

Table 1 Groundwater extraction rate assigned to each exploitation zones for the three exploitation scenarios simulated with the numerical model. The mean and maximum rates correspond to the overall historical level of MRA exploitation, whereas the ultimate rate corresponds to the maximum historical rate within each zone.

MRA exploitation zone	Scenario 1 (Mm^3/y)	Scenario 2 (Mm^3/y)	Scenario 3 (Mm^3/y)
Zone 1	0.311	0.598	0.603
Zone 2	0.019	0.026	0.056
Zone 3	0.111	0.211	0.227
Zone 4	0.220	0.389	0.655
Zone 5	0.028	0.041	0.064
Zone 6	0.471	0.805	0.888
Municipal wells	0.16	0.17	0.17
Total extraction rate in Domain	1.160	2.070	2.493
Total extraction rate in subdomain	0.963	1.564	1.954
Total extraction over 108 years (Mm3)-Domain	142.1	241.9	287.6
Total extraction over 108 years (Mm3)-Subdomain	104	169.8	211.2

3.4 Numerical model calibration criteria

Calibration of the numerical model was based on a set of quantitative and qualitative criteria. Thus, hydraulic heads measured in wells, conceptual direction and magnitude of groundwater fluxes as well as the extent of artesian areas were used to guide model calibration as discussed below.

There is very limited information related to the pre-development state of the aquifer. The steady-state calibration dataset consists of hydraulic heads (or calibration targets) produced from historic potentiometric surfaces of the MRA that are considered as representative of a steady-state condition not significantly affected by exploitation. Moreover, qualitative information describing the state of the aquifer at the beginning of the MRA exploitation was used. In Montana, the available potentiometric surface is from Pétré (2016). This map is actually a composite map of historical potentiometric maps from Levings (1982) in south-east Montana, Tuck (1993) in the Sweet Grass Hills area and Zimmerman (1967) in south-west Montana. Although these maps have been drawn after years of groundwater exploitation, it was assumed that they represented a condition similar to predevelopment. Indeed, the south-west area in Montana appears to have stable groundwater levels based on monitoring wells completed in the MRA. Besides, this area is likely under the influence of active recharge due to its higher transmissivity and closer proximity to the outcrop of the aquifer where direct recharge can occur (Figs. 4c and ESM1). In south-east Montana, the investigation carried out in the present study indicates that the magnitude of water use for oil and gas activity is low, except in the extreme south-east corner of the study area (Folnagy A.J.B., Montana Department of Natural Resource Conservation, personal communication). Eleven water level measurements from monitoring wells, mostly located in the outcrop area of the MRA in Montana, were added to the calibration dataset.

In Alberta, the same steady-state hypothesis was formulated in the area south of the Milk River, where it is assumed that the groundwater use is minor compared to what is found north of the river. Furthermore, this area receives recharge from the outcrop and subcrop areas that is not intercepted yet by the Milk River. The potentiometric maps used in Alberta are from Meyboom,

(1960) and Toth and Corbet, (1986), who reinterpreted Meyboom's data by better considering the surface topography and the potential effect of buried valleys. Simulated heads will be compared to both potentiometric interpretations. Such model calibration to groundwater levels could not be done in the area north of the Milk River, which has been subjected to intensive exploitation and does not have significant renewal from recharge in the outcrop/subcrop of the MRA due to the interception of groundwater by the Milk River.

A dataset of observation points was defined by randomly selecting points from the interpolated potentiometric surfaces that were interpolated beforehand within the model domain. As shown in Fig. 6, 132 observation points were defined in northern Montana and 80 points in Alberta (south of the Milk River). These observation points are assigned in the model within the layer at the centre of the Milk River Formation.

The discharge mechanism of the MRA through cross-formational flow has been highlighted in the conceptual model of the aquifer Pétré et al. (2016). The direction and magnitude of these cross-formational flows previously estimated are thus used here as a calibration criterion. More specifically, the upward flow component from the MRA to surficial sediments in the vicinity of the bedrock valleys was estimated to be between 4.0×10^2 to 4.0×10^5 m^3/y. Another cross-formational flow directed downward from the MRA through the Colorado Group and to the Bow Island Sandstone was also defined and estimated to be between 8.0×10^3 to 8.0×10^5 m^3/y.

Qualitative information on the occurrence of artesian conditions in the MRA provides an indication of the state of the pre-exploitation system. Previous studies indicate that nearly all the wells drilled in the MRA in southern Alberta were flowing in the pre-exploitation system (Borneuf, 1976; Hendry et al., 1991; Phillips et al., 1986). (Dowling, 1917) defined the flowing artesian limit in southern Alberta (Fig. 6). The steady-state model should thus represent this flowing artesian area and be consistent with Dowling's (1917) delineation. Although the magnitude of artesian conditions was not quantified in the past, four recent pressure measurements in the flowing area are available Pétré et al. (2016). It is assumed that under pre-development conditions, the hydraulic heads at these locations would have been greater than the present-day observations.

3.5 Adjustments of boundary conditions and hydraulic parameters

During the calibration process, the following modifications were made to improve the match between observed and simulated hydraulic heads. The density of the surface drainage was first adjusted locally during the calibration process. It was increased in a poorly drained area in the central part of southern Alberta and decreased north of the Etzikom coulee to better represent the observed spatial distribution of the flowing artesian area. These modifications imply that groundwater discharge to surface drainage from the MRA and through the overlying aquitard exerts an important control on hydraulic heads (and artesian conditions) in the MRA. Such discharge, while being relatively diffuse, could still be largely controlled by the presence of surface drainage representing low topography areas. Conversely, this could also mean that surface drainage partly reflects the discharge of groundwater originating from the MRA. This adjustment is in agreement with the observation from (Meyboom, 1960) who identified strong flowing wells along the main coulees.

In the Milk River canyon area, the value of the specified head boundary condition was adjusted as the resolution of the DEM representing the model surface elevation did not allow the proper representation of the 150-m deep and 1500 m-wide canyon (Beaty, 1990). The specified head was thus set to 30 m below land surface (as defined for the DEM and numerical model) to correctly represent the incision of the Milk River canyon and to increase its effect on groundwater interception, which led to a better representation of observed potentiometric conditions. This adjustment provided a better fit with the calibration target, suggesting that the Milk River Canyon is an important feature in the discharge mechanism of the MRA.

Table 2 summarizes the initial ranges of K values and vertical anisotropy for each hydrostratigraphic units and their final values that provided the best match between the numerical model and calibration criteria. A few new hydraulic tests recently conducted in the south-eastern part of the study area in Montana indicate that K of the Milk River/Eagle Formation is higher than indicated by ESM1 (A. Folnagy, Montana Department of Natural Resource Conservation, personnal communication). To take into account these new observations, K of the MRA in the south-east corner of the study area was locally increased by a multiplication factor, adjusted during the calibration process. The numerical model should thus better represent K of the MRA. Miller and Norbeck (1996) give a K value for the Pakowki/Claggett aquitard in the East Butte area (the eastern Butte of the Sweetgrass Hills) that is much higher than the uniform value used for this geological unit. This higher value of 9×10^{-8} m/s was assigned to the Pakowki/Claggett Formation in the East Butte area. It provided a better match of hydraulic heads in this area, suggesting that a zonation of K of the Pakowki/Claggett aquitard is necessary. This modification indicates that this aquitard probably does not have spatially uniform hydraulic properties over the study area but available data do not allow the definition of the spatial distribution of K.

Table 2 Estimated ranges of hydraulic conductivity and vertical anisotropy for each hydrostratigraphic units and their final (calibrated) values

Hydro-statigraphic units	**Horizontal hydraulic conductivity K_x (m/s)**	**K anisotropy (K_x/K_z)**	**Sources**	Final values	
				Horizontal hydraulic conductivity K_x (m/s)	**K anisotropy (K_x/K_z)**
Surficial sediments (till)	7×10^{-8}	1	Robertson (1988); Hendry and Buckland (1990)	7×10^{-8}	1
Belly/Judith River Formation	9×10^{-8}-8.8×10^{-7}	10-10^4	Hendry and Buckland (1990); Anna (2011)	5×10^{-7}	10^3
Pakowki/ Claggett Formation	10^{-9}-10^{-11}	5	Swanick (1982); Hendry and Schwartz (1988)	1×10^{-9} (9×10^{-8} in East Butte area)	5
Milk River Formation	Spatial distribution from	10	Pétré et al. (2016)	Spatial distribution in	10

	Fig.5			ESM1 (factor 50 in south-east Montana)	
Colorado Group	10^{-9}-10^{-12}	10	Toth and Corbet (1986); Robertson (1988); Hendry and Buckland (1990)	1×10^{-10}	10
Bow Island Sandstone	10^{-6}-10^{-8}	10	(Schwartz et al., 1981)	5×10^{-7}	10
Bedrock valleys	10^{-3}-10^{-4}	1	Cummings et al. (2012b)	1×10^{-6}	1

4. Results

4.1 Hydrogeological model calibration

Model calibration was carried out by trial-and-error with the objective of obtaining the best fit between simulated and observed heads at the 212 calibration targets as well as a proper representation of the artesian conditions in the MRA. The calibration performance was quantified by calculating the root mean square error (RMSE), the correlation coefficient (r) for each calibration zone and the scaled RMSE (Table 3). The combination of a small RMSE and high r indicates a satisfying calibration. Furthermore, the scaled RMSE should be below the threshold value of 5%, as recommended by Anderson and Woessner (1992) and Giambastiani et al. (2012).

In Montana, good calibration is achieved in the south-west where the lowest RMSE (30.8 m) and the highest correlation coefficient (0.89) are found. In southern Alberta, south of the Milk River, the best calibration is achieved following the Toth and Corbet (1986) interpretation of the potentiometric surface, with a RMSE of 28.4 m and a satisfying r of 0.89. As the Toth and Corbet (1986) interpretation of the potentiometric surface mimics the topography, this suggests that the topography exerts a major influence on the pattern of the potentiometric surface. Figure 8b shows the effect of both Toth and Corbet's (1986) and Meyboom's (1960) interpretations on the calibration performance. This result illustrates the uncertainty of the reference potentiometric map as several interpretations lead to different calibration performance. However, the model indicates that the Toth and Corbet (1986) interpretation of the potentiometric map appears to be the most hydraulically plausible.

In southern Alberta and the south-western part in Montana, the scaled RMSE values are below or close to the 5% limit (4.9 and 5.3%). The other two calibration zones in the south-eastern part of the study area in Montana and in the Sweet Grass Hills area show lower correlation coefficients (0.85 and 0.83) and have higher RMSE (44.4 and 35.9), which implies poorer calibration. The scaled RMSE value are higher than the 5% limit in these calibration zones (7.7 and 6.2%).

The calibration is poorer in the south-east area in Montana because this area combines the highest uncertainty in the geological model (due to a lack of geological data) and the highest uncertainty in the reference water levels. Indeed, the water levels are derived from a regional potentiometric map at the Montana-state level (Levings, 1982). The steep topography in the Sweetgrass Hills area explains the difficulty to obtain a good calibration in this calibration zone.

A detailed analysis of the levels of calibration for each calibration zone is presented in the electronic supplemental material ESM2. The comparison between contours maps of observed and simulated heads shows a good representation of the observed radial groundwater flow pattern as indicated in the electronic supplemental material ESM3. The groundwater divide north of Cut Bank is also satisfactorily reproduced by the model. The scatter plot of simulated versus measured heads is shown in Fig. 7a. The model tends to overestimate the simulated heads in the south-eastern part of the study area in Montana and in southern Alberta.

Table 3 Hydraulic head calibration performance of the groundwater flow model in the calibration zones

Calibration Zone	*RMSE (m)*	*Correlation coefficient (r)*	*Scaled RMSE (%)*
Montana, south-west	30.8	0.89	5.3
Montana, Sweet Grass Hills	35.9	0.83	6.2
Montana, south-east	44.4	0.85	7.7
Alberta, south of the Milk River (Toth and Corbet 1986)	28.4	0.89	4.9
Alberta, south of the Milk River (Meyboom 1960)	41.3	0.85	7.1

Simulated flowing artesian conditions in the MRA are mostly located in the northern part of the study area, along the Chin and Etzikom Coulees, in the vicinity of Lake Pakowki and following the Milk River reach in the north-eastern part of the study area in Montana (ESM4). In Alberta, these locations are consistent with the delineation of the artesian zone from Dowling (1917) and the observation of strongly flowing wells in the coulees (Meyboom, 1960). Approximatively 62% of the MRA nodes located in the flowing artesian area defined by Dowling (1917) are indeed simulated as flowing nodes. At the four locations where recent pressure measurements were obtained (ESM4), the magnitudes of the simulated artesian conditions are higher than the measurements. This result was expected as pre-development artesian conditions must have had a greater intensity than the present-day conditions. The numerical model thus successfully represents the location and magnitude of the flowing artesian area in Alberta. In south-east Montana, the simulated artesian conditions are located along the southern reach of the Milk River and Sage Creek. The presence of artesian conditions at this location has not been documented in previous studies. It is however plausible due to the combination of confined conditions in the MRA and lower elevations, where the river is more incised, that could result in strong artesian conditions, as observed in Alberta. Nevertheless, high magnitude in artesian conditions locally is most probably due to the low-permeability Pakowki Formation which outcrops along the Milk River due to uncertainties in the geological model in this area. Besides, the high uncertainty in K of the MRA in this area can also explain these large values.

In order to assess the performance and uncertainty of the model relative to changes in calibration parameters, a parameter sensitivity analysis was carried out (electronic supplemental material ESM5). This analysis shows that the calibrated parameters provide a balance between hydraulic heads calibration and the representation of artesian conditions. This analysis also showed that the model is very sensitive to the recharge rate and that the most plausible recharge value could only be between the calibrated value and a value 1.5 times greater. The determination of the actual recharge rate is critical in addressing the sustainability of the MRA exploitation.

4.2 Simulation of groundwater extraction scenarios

The steady-state calibrated model was used to simulate natural conditions without groundwater exploitation as well as three groundwater extraction scenarios (Table 1), as presented in section 3.3 “Groundwater use evaluation in southern Alberta”. One indicator of the long-term effect of groundwater extraction is the simulated steady-state regional drawdown compared to natural conditions that is caused by the three exploitation scenarios over Alberta (Fig. 8): a) mean groundwater extraction, b) maximum groundwater extraction, and c) ultimate groundwater extraction corresponding to the maximum historical rate in each exploitation zone (Fig. 5).

For scenario 1 with mean groundwater extraction rate, drawdowns between 2 and 10 m are simulated in the central part of the domain where a large proportion of the groundwater pumping is found. The drawdown is also higher in the vicinity of the main municipal wells who were represented individually in the numerical model, notably in Foremost. These drawdowns have led to a loss of 9% of artesian conditions compared to natural conditions.

In the case of scenario 2 representing the maximum groundwater extraction rate, higher drawdown is simulated (5 to 20 m) in the central and north-eastern parts of the domain. In that case, artesian conditions decrease by 15% compared to natural conditions. Drawdowns of about 122 m in the Foremost area approach the top of the MRA.

In scenario 3 representing the ultimate MRA exploitation rate in each zone, simulated drawdowns increase dramatically in the central and north-eastern part of the domain where their range is from 10 to 30 m in the central part. The loss of artesian conditions is 21% compared to the natural conditions. The simulated local drawdown of the Foremost well reaches the top of the MRA in scenario 3.

Since groundwater extraction is spatially distributed in the numerical model, the simulated local drawdown is minimized compared to the actual drawdown that would be observed for a specific water well. To assess the impact of groundwater extraction on the economic exploitability of the MRA, it is necessary to take into account the additional local drawdown at extraction wells, except for the main municipal wells that are already represented individually in the model. Table 4 shows the local expected drawdown for the range of transmissivity values of the MRA. The drawdown was calculated using 50% of a typical pumping rate of 7500 m^3/y for domestic and stock use (Alberta Water Act, 2000), a well casing radius of 0.06 m and the transmissivity data of the MRA from Meyboom (1960) and Persram (1992). This result indicates that an additional few meters of drawdown could be expected locally, depending on the transmissivity and the actual pumping rate.

Table 4 Calculated local drawdown at exploitation wells for the range of MRA transmissivity values in Alberta

T (m^2/s)×10^{-5}	*20*	*2*	*9*	*0.52*
Local drawdown (m)	64	6	1	0

Fig. 8d presents the approximate drawdown derived from local water wells between the late 1950s and the late 1990s (AGRA Earth and Environmental Limited, 1998). Drawdowns may be higher than those simulated in the model due to local effects. However, the order of magnitude as well as the spatial distribution of the drawdown are similar. This suggests that the system rapidly equilibrates with respect to the period of exploitation. Therefore, it seems acceptable to assess the sustainability of the MRA exploitation under steady-state conditions.

The water level drawdown induces a loss of storage in the MRA. It is possible to estimate the loss of storage from the mean simulated drawdown as shown in Table 5. With increasing groundwater abstraction, the loss of storage increases from 4.1 Mm^3 to 8.3 Mm^3 and from 12.4 to 24.8 Mm^3, using a storage coefficient of 1×10^{-4} and 3×10^{-4} respectively. This range of value in the storage coefficient of the MRA is derived from local estimates from pumping tests in the Foremost and Sweet Grass Hills area (Meyboom 1960, DNRC, unpublished report).

Table 5 Loss of groundwater storage in the MRA in Alberta under the three simulated exploitation scenarios

		Scenario 1	Scenario 2	Scenario 3
Mean drawdown (m) in the MRA		4.1	6.5	8.2
Loss of storage (Mm^3)	S= 1×10^{-4}	4.1	6.5	8.3
	S= 3×10^{-4}	12.4	19.6	24.8

4.3 Water balance

The water flux into the model is controlled by the imposed recharge (Fig. 4c), thus the water balance of the full model is the same for simulated natural conditions, as well as for the three exploitation scenarios The entire model domain has a simulated annual groundwater flow of 243 Mm^3/y (1 Mm^3 = $1x10^6$ m^3) and all models converged with a water imbalance of <0.01%.

Water balances were obtained from the numerical model under natural conditions as well as for the three exploitation scenarios. These water balances considered a subdomain of the numerical model in the area north of the Milk River and east of the town of Warner, where the majority of groundwater exploitation takes place. The use of this subdomain also allows the comparison of the numerical model water balance with the one related to the conceptual model estimated by Pétré et al. (2016). In order to assess the impact of the MRA exploitation on the entire regional flow system, the water balance was first established for the regional flow system (Table 6) and then specifically for the MRA (Table 7).

Table 6 Water balance of the entire flow system in Alberta under steady state conditions

Aquifer system water balance (north of the Milk River) m^3/d	Natural conditions	Mean extraction rate	Maximum extraction rate	Ultimate extraction rate
Recharge	21739	21739	21739	21739
Discharge to seepage locations	-21305	-19526	-17262	-16261
Discharge to Bow Island perimeter nodes	-1109	-1082	-1064	-1045
Net flux to(-)/from(+) the MRA	0	-2086	-3695	-4593
Flux from the western limit of the subdomain	98	112	124	124
Flux beyond the Milk River in other units	189.5	309.81	392.53	424.83
Water balance error	-388	-534	234	389
Water balance error (% of total recharge)	-1.8	-2.5	1.1	1.8
Aquifer system water balance (north of the Milk River) - Relative to the total recharge (%)				
Recharge	100.00	100.00	100.00	100.00
Discharge to seepage locations	-98.00	-89.82	-79.41	-74.80
Discharge to Bow Island perimeter nodes	-5.10	-4.98	-4.89	-4.81
Net flux to(-)/from(+) the MRA	0.00	-9.60	-17.00	-21.13
Flux from the western limit of the subdomain	0.45	0.52	0.57	0.57
Flux beyond the Milk River in other units	0.87	1.43	1.81	1.95

For the entire flow system, the water balance under exploitation sees a reduction in discharge to seepage locations that mostly compensates the groundwater abstracted from the MRA. In scenario 1 (mean exploitation), this reduction in seepage is in the order of 8%, but it could reach about 24% in scenario 3. Besides, the net flux to/from the MRA increases up to 4593 m3/d in scenario 3, which correspond to 21% of the total recharge. The other components of the budget do not change significantly under exploitation.

At the MRA scale, the water balance components are depicted in Table 7 and Fig. 9 and further described below:

Transboundary fluxes and effective MRA recharge. The simulated transboundary flux is 16,320 m^3/d (5.96 Mm^3/y), while in the conceptual model it is 24,657 m^3/d (9.0 Mm^3/y) (Pétré et al., 2016). The groundwater flux transmitted through the international border also corresponds to the effective recharge rate of the MRA by assuming that this flux is solely due to the portion of the potential recharge that actually reaches the aquifer. In the numerical model, an effective recharge rate of 10 mm/y was applied on the outcrop area of the MRA to produce the simulated transboundary flux. Besides, the steady-state hypothesis in the area south of the Milk River is confirmed since the recharge flux is greater than the groundwater extraction and the simulated drawdowns are small in this area. Under exploitation, the transboundary flux does not change significantly.

Table 7 Water balance of the MRA in Alberta under steady state conditions

	Natural conditions	Scenario 1	Scenario 2	Scenario 3
Transboundary flux	16,320	16,390	16,448	16,459
Flux beyond the Milk River	1,414	1,497	1,555	1,576
Flux from overlying units	177	2,383	3,761	4,674
Flux to the bedrock valleys	-684	-297	-66	-81
Flux to the underling aquitard	-896	-861	-838	-816
Groundwater use	0	-2,639	-4,307	-5,357
Budget error	11	82.65	105.74	-3.87
Budget error (%)	0.70	2.13	1.99	-0.06

Ground water flow interception by the Milk River. The simulated flux intercepted by the Milk River and its tributaries is about 14,906 m^3/d (5.44 Mm^3/y). This value represents 91.3% of the incoming groundwater flux flowing from the south of the Milk River in the MRA. The numerical model thus shows that the Milk River is effectively the main discharge feature of the MRA in terms of magnitude. The groundwater flow interception slightly decreases with increasing groundwater use. Indeed, the simulated flux transmitted beyond the Milk River increases from 1,414 m^3/d (0.52 Mm^3/y) in natural conditions to 1,576 m^3/d (0.58 Mm^3/y) in scenario 3.

Cross-formational flow (vertical leakage). In southern Alberta, north of the Milk River, the numerical model simulates a downward vertical flow of 896 m^3/d (0.33 Mm^3/y) (directed from the MRA to the Colorado Group) and an upward flow of 684 m^3/d (0.25 Mm^3/y) along the bedrock valleys (directed from the MRA to the Pakowki/Claggett Formation). This discharge mechanism of the MRA was proposed by Borneuf (1976) and Toth and Corbet (1986) but this flux had not previously been quantified. Both cross-formational flow values are in the range of estimates from the conceptual model formulated by (Pétré et al., 2016). Under exploitation of the MRA, the cross-formational flow decreases. For instance, the flow to the bedrock valley decrease of about 89% in scenario 3 in comparison with natural conditions whereas there is an 8% decrease in the downward flow to the underlying aquitard.

Groundwater inflow from the overlying units. The MRA receives a groundwater inflow of about 177 m^3/d (0.07 Mm^3/y) from overlying units, especially in the vicinity of the topographic highs (Cypress Hills). This result supports the statement from Toth and Corbet (1986), according to which the MRA receives groundwater inflow from topographic highs in the study area. Under exploitation of the MRA, the inflow from the overlying units compensate for most of the groundwater extraction and reaches up to 4,674 m^3/d (1.7 Mm^3/y) in scenario 3.

Groundwater storage in the MRA

The estimated volume of water stored in the MRA ranges from 100 to 300 Mm^3, using the range of values for the storage coefficient of the MRA (1×10^{-4} to 3×10^{-4}) and knowing the total volume of the MRA in the budget subdomain (1×10^{12} m^3). The previous estimate from the conceptual model was about 380 Mm^3 of water stored in the MRA, using Meyboom's value for storage coefficient (3×10^{-4}).

As mentioned in section 3.4 (Numerical model calibration criteria), the numerical groundwater flow model was calibrated in a way that the direction and magnitude of the groundwater budget components are in agreement with the conceptual model. Therefore, the comparison between the simulated and estimated values under natural conditions shows that the conceptual model is hydraulically plausible.

Particle tracking gives a representation of the groundwater flow pattern within the system, ESM6 shows both forward and backward particle tracking starting from the central nodes in the MRA unit .

Under natural conditions, the MRA discharges to the surface especially along the coulees and bedrock valleys as well as through the underlying Colorado Aquitard (ESM6a). Under exploitation of the MRA (ESM6 b) c) and d)), the groundwater flow patterns significantly change in the entire flow system. The discharge to the surface considerably decreases and the travel time to the Colorado Aquitard increases, which illustrates the concept of capture to compensate for the groundwater withdrawals in the MRA.

The quantification of the sources of groundwater abstracted over the exploitation period is a crucial question in understanding how the MRA and the entire flow system adapt to groundwater extraction. Table 8 provides an estimation of the sources of the groundwater abstracted over the 108-year exploitation period. The first two columns correspond to a transient period of 108 years during which an inflow from the storage depletion (estimated in Table 5) is considered. The groundwater flow coming from the change in flow patterns in and out of the MRA is obtained by subtracting the decrease in storage and the flux transmitted beyond the Milk River to the total exploitation. The range of plausible storage coefficient values is considered in this calculation. The last two columns of Table 8 describe the conditions simulated in the steady-state model and correspond to the new equilibrium reached by the aquifer system.

Under scenario 1 and using a storage coefficient of $1x10^{-4}$, the loss of groundwater storage in the MRA (4.1 Mm^3) has provided 4 % of the water abstracted from the MRA over 108 years. This loss in storage represents about 4% of the total water stored in the MRA without exploitation (100 Mm^3). Direct inflow beyond the Milk River has contributed 59 Mm^3 (57%) of groundwater abstraction, and changes in flow patterns in and out of the MRA have contributed 40.9 Mm^3 (39%). However, under the new steady-state conditions of mean MRA exploitation this change in flow patterns represent 46% of water abstraction from the MRA. Under scenario 2 and 3 the loss of groundwater storage remains in the same proportions relatively to the total water abstracted whereas the contribution of the changes in the flow patterns in and out of the MRA increases. The volume of direct inflow beyond the Milk River does not change significantly with increased groundwater abstraction but its contribution increase as the flow system adjust to the pumping.

Table 8 Sources of the abstracted groundwater in Alberta over 108 years under the three simulated exploitation scenarios. In the transient budget, the two figures in the decrease in storage and the proportion in changes in and out from the MRA corresponds to calculations using a storage coefficient value of 1×10^{-4} and 3×10^{-4}.

Mean extraction rate (scenario 1)	Transient conditions over 108 years		New equilibrium conditions (steady-state)	
	Volumes (Mm^3)	Proportions (%)	Rate (m^3/d)	Proportions (%)
Total extraction	104.0	100	2,639.4	100.0
Decrease in storage	4.1/12.4	4.0/11.9	0	0.0
Flux beyond the Milk River	59.0	56.7	1,497.0	-56.7

Changes in out/inflow of MRA	40.9/32.6	39.3/31.4	1,225.1	-46.4

Maximum extraction rate (scenario 2)	**Transient conditions over 108 years**		**New equilibrium conditions**	
Total extraction	169.8	100.0	-4,307	100.0
Decrease in storage	6.5/19.6	3.9/11.6	0.0	0.0
Flux beyond the Milk River	61.3	36.1	1,555.4	-36.1
Changes in out/inflow of MRA	101.9/88.8	60.0/52.3	2,857.0	-66.3

Ultimate extraction rate (scenario 3)	**Transient conditions over 108 years**		**New equilibrium conditions**	
Total extraction	211.2	100.0	-5,357	100.0
Decrease in storage	8.3/24.8	3.9/11.7	0.0	0.0
Flux beyond the Milk River	62.1	29.4	1,576.0	-29.4
Changes in out/inflow of MRA	140.8/124.3	66.7/58.8	3,777.0	-70.5

Using a storage coefficient of 3×10^{-4}, the contribution from the loss of storage over 108 years increases to 12% in all three scenarios. As previously stated, the total volume of water stored in the MRA would be about 300 Mm^3 in that case which means that the percentage of storage loss relative to the total volume of water stored in the MRA is the same (4%) as in the previous case ($Ss=1\times10^{-4}$).

5. Discussion

5.1 Model limitations

The numerical groundwater flow model developed in the present study is a simplification of the real aquifer system. The following limitations and sources of uncertainties should be taken into consideration when examining model results.

A first source of uncertainty lies in the underlying geological model, which constitutes the basis of the groundwater flow model. The error associated with the geometry, thickness and structure of the hydrostratigraphic units are reflected in the groundwater flow model. This is especially true in the south-east part of the model in Montana, where the geological data were sparse (Pétré et al., 2015), thus increasing the degree of uncertainty in the geometry of the geological units.

The limits of the geological model further constrain the groundwater flow model, as it does not extend in the Big Sandy Creek and Bear Paws Mountains areas in Montana due to a lack of geological data. Therefore, the hydraulic head contours do not completely reflect the south-west/north-east orientation of the potentiometric low along the Big Sandy Creek, which was highlighted in the conceptual model. Collection of new data in this area would allow a better representation of the groundwater flow pattern in the south-east corner of the study area.

The assumption that the potentiometric maps in Montana and south of the Milk River in Alberta are representative of a steady-state situation might not be correct everywhere and could explain the tendency towards overestimation of simulated heads south of the Milk River in Alberta and in the south-east Montana. The south-east area in Montana combines the highest error associated with the hydraulic conductivity of the MRA and a higher uncertainty concerning the geometry of the geological unit. Thus, this is the less reliable area in the model domain.

The non-uniqueness problem occurs when different sets of parameters give equally good models, in terms of matching the observations. The manual trial-and-error calibration done in the present study does not rule out this issue. However, to address the non-uniqueness problem, the spatial distribution of hydraulic conductivity of the MRA was obtained from measured data and the hydraulic conductivity of the other hydrostratigraphic units was limited to a range considered close to reasonable values. Besides, the sensitivity analysis (ESM5) shows that the values used in the model lead to minimal errors and correspond to an optimal model calibration.

Another limitation of the model is that the steady-state simulations do not allow the determination of the storage dynamics over time as well as the time required to reach an equilibrium. Finally, the determination of the loss of storage from the confining units cannot be addressed in this steady-state model.

5.2 Implications for groundwater management

The results of the steady-state model of the regional groundwater flow system encompassing the MRA have some implications on the management of the groundwater resource. As seen before, the numerical model shows that the conceptual model of the MRA is hydraulically plausible by successfully representing the location of the groundwater divide in Montana as well as the transboundary fluxes and the main components of the groundwater budget. Thus, the numerical model confirms that the MRA is an internationally shared groundwater resource, with two transboundary fluxes flowing from the recharge area in Montana to the north in Alberta.

It seems therefore appropriate to consider the implementation of a joint management of this shared resource between Canada and the USA. Both the numerical and conceptual models of the MRA allow the delineation of the proper management unit for such a transboundary management. The appropriate management unit would be comprised between the north of the groundwater divide in Montana and the south of the Canadian reach of the Milk River and Verdigris Coulee (also defined as “zone 1a” in Pétré et al. (2016)).

As described in the “water balance” section, due to the major interception of the incoming groundwater flow by the Milk River, the flux north of the Milk River is quite low (1,096 m^3/d). This groundwater flux represents the main external groundwater renewal mechanism of the MRA. Thus, the area north of the Milk River only receives a small portion of the main recharge flux from the MRA outcrop area whereas the area south of the Milk River benefits from the totality of the transboundary flux coming from the south.

The numerical simulation under natural conditions showed that the MRA is part of a large regional flow system involving important flow through the confining units. The numerical simulation of this flow system supports conceptual work from Toth (1963) and Freeze and Witherspoon (1966a, 1966b). Groundwater withdrawals in the MRA has a considerable impact on the entire flow system. It is then necessary to consider the flow system as a whole to assess the sustainability of the MRA exploitation. The flow system can adapt to large exploitation levels in the MRA and reach a new equilibrium. However, this new equilibrium implies significant impacts such as major drawdowns locally and a decrease of the water flow emerging to the surface. The exploitation of the MRA leads to a decrease in groundwater storage. This loss of storage is estimated by comparing conditions with and without exploitation but its transient evolution cannot be followed due to the steady-state regime. It is possible that a large proportion of this loss of storage will not be recoverable (Konikow and Neuzil, 2007). Groundwater use scenario 2 corresponding to the maximum exploitation rate thus possibly better represents the permanent loss of storage in the MRA.

The average historical level of exploitation of the MRA (scenario 1) appears to be sustainable whereas scenario 3 leads to major drawdowns that would prevent the MRA exploitation, or make it very expensive. The loss of artesian conditions would either require installing water pumps where they were not required before or installing pumps deeper in wells, which could be challenging economically and technically. Quality issues may also arise since the water coming from the overlying units are more mineralized than water from the MRA.

Scenario 2 corresponds to intermediate conditions and would represent a limiting case of the MRA exploitation as it still results in important regional drawdowns and captures a large proportion of the water which originally flows back to the land surface.

6. Conclusion

A steady-state numerical model of the regional groundwater flow system comprising the transboundary Milk River Aquifer (MRA) was developed with the objective of understanding the impact of major and long-term exploitation on the entire aquifer system and to identify the processes controlling the sustainable exploitation of the MRA. Results from this work has implications on our general understanding of large flow systems and provides specific results on the sustainable exploitation conditions of the MRA. Steady-state simulations of three groundwater extraction scenarios demonstrate that groundwater withdrawals cause changes in the entire flow system. Indeed, results indicate that loss of storage, less outflow and more inflow supplied the groundwater that was extracted, illustrating the important role of capture in a regional groundwater flow system. The quantification of cross-formational flow through aquitards showed that the MRA is not an isolated hydrogeological unit but is rather part of a large groundwater flow system. Sustainability of regional aquifers should therefore be defined by taking into account the entire flow system. Overall, this work makes an important contribution to major hydrogeological questions related to regional flow, especially through the aquitards, as well as the impact of the exploitation on the flow system and the long-term reduction of groundwater storage in a regional aquifer. Although this study provides interesting and relevant results, the steady state numerical modelling did not allow the representation of storage dynamics over time as well as the time required to reach an equilibrium.

Concerning the specific findings relative to the MRA sustainable exploitation, results show that the numerical model is in agreement with the previously formulated conceptual model and thus supports its hydraulic plausibility. Then, the mean historical extraction rate (scenario 1) appears sustainable because the regional groundwater flow system can adapt and is able to reach a new equilibrium. In contrast, the highest level of exploitation (scenario 3) does not seem sustainable as it leads to dramatic drawdowns in the MRA and an important capture of cross-formational flow. This level of exploitation would endanger the technical and economical exploitation of the MRA and could possibly threaten the beneficial use of surface water from the coulees. The intermediate scenario 2 corresponds to a borderline condition which should not be exceeded. The numerical model also illustrates that the MRA is a transboundary groundwater resource. Thus, an internationally shared management strategy of the MRA would be warranted, especially in the area comprised between the groundwater divide in Montana and the southern reach of the Milk River in Alberta. Finally, future modelling would have to accompany management decisions to assess future exploitation scenarios.

Acknowledgements

This work was supported by the Groundwater Geoscience Program of the Geological Survey of Canada within the MiRTAP (Milk River Transboundary Aquifer Project). We are grateful to Nicolas Benoît and Daniel Paradis (Geological Survey of Canada) for their constructive discussions at early stages of the development of the numerical model. This is a Land and Minerals Sector of Natural Resources Canada contribution 20190019 for the second author.

7. References

AGRA Earth and Environmental Limited, 1998. Evaluation of depletion of the Milk River aquifer. AGRA Earth & Environmental, Edmonton.

Alberta Water Act, 2000. Revised Statutes of Alberta 2000 Chapter W-3, Province of Alberta. http://www.qp.alberta.ca/documents/Acts/w03.pdf. Accessed in October 2018 [WWW Document].

Alwathaf, Y., Mansouri, B.E., 2012. Hydrodynamic modeling for groundwater assessment in Sana'a Basin, Yemen. Hydrogeol J 20, 1375–1392. https://doi.org/10.1007/s10040-012-0879-6

Anderson, M.P., Woessner, W.W., 1992. Applied groundwater modeling: simulation of flow and advective transport. Gulf Professional Publishing.

Anna, L.O., 2011. Effects of groundwater flow on the distribution of biogenic gas in parts of the northern Great Plains of Canada and United States (No. SIR-2010-5251). U.S. Geological Survey.

Beaty, C.B., 1990. Milk River in Southern Alberta: A Classic Underfit Stream. Canadian Geographer / Le Géographe canadien 34, 171–174. https://doi.org/10.1111/j.1541-0064.1990.tb01265.x

Bordeleau, G., Martel, R., Schäfer, D., Ampleman, G., Thiboutot, S., 2008. Groundwater flow and contaminant transport modelling at an air weapons range. Environ Geol 55, 385–396. https://doi.org/10.1007/s00254-007-0984-3

Borneuf, D.M., 1976. Hydrogeology of the Foremost Area. Alberta Research Council, Earth Sciences Report 1974-04. Alberta, Alberta Research Council, Edmonton, Alberta.

Climate Canada, 2015. Canadian Climate Normals. 1981-2010 Climate Normals and Averages. [WWW Document]. URL http://climate.weather.gc.ca/climate_normals/index_e.html

Colton RB, Lemke RW, Lindvall RM (1961) Glacial map of Montana east of the Rocky Mountains. US Geological Survey. IMAP 327, Scale 1:500,000

Cummings, D.I., Russell, H.A., Sharpe, D.R., Fisher, T.G., 2012a. Buried-valley aquifers in the Canadian Prairies: geology, hydrogeology, and origin. Canadian Journal of Earth Sciences 49, 987–1004.

Cummings, D.I., Russell, H.A.J., Sharpe, D.R., 2012b. Buried-valleys and till in the Canadian Prairies: geology, hydrogeology, and origin. Geological Survey of Canada, Current Research 2012-4. https://doi.org/10.4095/289689

Diersch, H.-J.G., 2014. FEFLOW: finite element modeling of flow, mass and heat transport in porous and fractured media. Springer.

Dowling, D.B., 1917. Southern plains of Alberta. Geological Survey of Canada, “A” Series Map 187A, 1917; 1 sheet, doi:10.4095/106740 (No. 1646).

Farvolden, R.N., Meneley, W.A., Lebreton, E.G., Lennox, D.H., Meyboom, P., 1963. Early contributions to the groundwater hydrology of Alberta. Alberta Res. Council Bull 12, 123.

Freeze, R.A., Witherspoon, P.A., 1966a. Theoretical analysis of regional groundwater flow: 1. Analytical and numerical solutions to the mathematical model. Water Resour. Res. 2, 641–656.

Freeze, R.A., Witherspoon, P.A., 1966b. Theoretical analysis of regional groundwater flow: 2. Effect of water-table configuration and subsurface permeability variation. Water Resour. Res 2, 641–656.

Gaur, S., Chahar, B.R., Graillot, D., 2011. Combined use of groundwater modeling and potential zone analysis for management of groundwater. International Journal of Applied Earth Observation and Geoinformation 13, 127–139. https://doi.org/10.1016/j.jag.2010.09.001

Giambastiani, B.M.S., Antonellini, M., Oude Essink, G.H.P., Stuurman, R.J., 2007. Saltwater intrusion in the unconfined coastal aquifer of Ravenna (Italy): A numerical model. Journal of Hydrology 340, 91–104. https://doi.org/10.1016/j.jhydrol.2007.04.001

Giambastiani, B.M.S., McCallum, A.M., Andersen, M.S., Kelly, B.F.J., Acworth, R.I., 2012. Understanding groundwater processes by representing aquifer heterogeneity in the Maules creek catchment, Namoi valley (New South Wales, Australia). Hydrogeology Journal 20, 1027–1044.

Government of Alberta, Alberta water for life, 2006. Water conservation and allocation guideline for oil field injection.

HCL consultants, 2004. County of Forty Mile No. 8, Parts of the South Saskatchewan River and Missouri River Basins.Regional Groundwater Assessment, Tp 001 to 013, R 05 to 14, W4M.

Hendry, J., Schwartz, F.W., Robertson, C., 1991. Hydrogeology and hydrochemistry of the Milk River aquifer system, Alberta, Canada: a review. Applied Geochemistry 6, 369–380. https://doi.org/10.1016/0883-2927(91)90037-P

Hendry, M.J., Buckland, G.D., 1990. Causes of Soil Salinization: 1. A Basin in Southern Alberta, Canada. Ground Water 28, 385–393. https://doi.org/10.1111/j.1745-6584.1990.tb02268.x

Hendry, M.J., Schwartz, F.W., 1988. An alternative view on the origin of chemical and isotopic patterns in groundwater from the Milk River Aquifer, Canada. Water Resour. Res. 24, 1747–1763. https://doi.org/10.1029/WR024i010p01747

IGRAC, 2015. International Groundwater Resources Assessment Center. Tranboundary Aquifer of the World 2015. Special edition for the 7th World Water Forum 2015. http://www.un-igrac.org/downloads.

Islam, M.B., Firoz, A.B.M., Foglia, L., Marandi, A., Khan, A.R., Schüth, C., Ribbe, L., 2017. A regional groundwater-flow model for sustainable groundwater-resource management in the south Asian megacity of Dhaka, Bangladesh. Hydrogeol J 25, 617–637. https://doi.org/10.1007/s10040-016-1526-4

Janos, D., Molson, J., Lefebvre, R., 2018. Regional groundwater flow dynamics and residence times in Chaudière-Appalaches, Québec, Canada: Insights from numerical simulations, Canadian Water Resources Journal / Revue canadienne des ressources hydriques, 43:2, 214-239, DOI: 10.1080/07011784.2018.1437370

Konikow, L.F., 2015. Long-term groundwater depletion in the United States. 53, 2–9.

Konikow, L.F., Leake, S.A., 2014. Depletion and capture: revisiting '"the source of water derived from wells"'. Groundwater 52 Focus Issue, 100–111.

Konikow, L.F., Neuzil, C.E., 2007. A method to estimate groundwater depletion from confining layers. Water Resources Research 43. https://doi.org/10.1029/2006WR005597

Lavigne, M.-A., Nastev, M., Lefebvre, R., 2010. Regional sustainability of the Chateauguay River aquifers. Canadian Water Resources Journal 35, 487–502.

Levings, G.W., 1982. Potentiometric-surface map of water in the Eagle Sandstone and equivalent units in the Northern Great Plains area of Montana (No. OFR-82-565). United States Geological Survey.

Meyboom, P., 1960. Geology and groundwater resources of the Milk River sandstone in southern Alberta. Research Council of Alberta.

Meyer, P.A., Brouwers, M., Martin, P.J., 2014. A three-dimensional groundwater flow model of the Waterloo Moraine for water resource management. Canadian Water Resources Journal/Revue canadienne des ressources hydriques 39, 167–180.

Michael, H.A., Voss, C., 2009. Controls on groundwater flow in the Bengal Basin of India and Bangladesh: regional modeling analysis. Hydrogeology Journal 17, 1561–1577. https://doi.org/10.1007/s10040-008-0429-4.

Miller, K.J., Norbeck, P., M., 1996. Ground-water evaluation of the East Butte of the Sweet Grass Hills, North-Central Montana. Montana Bureau of Mines and Geology Open-File Report 351.

NOAA, 2015. National Centers for Environmental Information. Data Tools: 1981-2010 Normals. [WWW Document]. URL http://www.ncdc.noaa.gov/cdo-web/datatools/normals

Okulitch, A.V., Lopez, D.A., Jerzykiewicz,T., 1996. Geology, Lethbridge, Alberta-Saskatchewan-Montana. Map NM-12-G. National Earth Science Series, Geological Atlas.

Pawlowicz, J.G., Fenton, M.M., Andriashek, L.D., 2007. Bedrock thalwegs, 1:2 000 000 scale (GIS data, line features),DIG 2007-0026,Alberta Geological Survey.

Persram, A.S., 1992. (draft report, unpublished): Hydrogeology of the Milk River Formation in Southern Alberta,Alberta Environmental Protection, Hydrogeology Branch,internal (draft) report.

Pétré, M.-A., 2016. Hydrogeological study of the Milk River transboundary aquifer (Canada-USA): geological, conceptual and numerical models for the sound management of the groundwater resource. (PhD Thesis). INRS- Centre Eau Terre Environnement, Québec, Canada.

Pétré, M.-A., Rivera, A., Lefebvre, R., 2015. Three-dimensional unified geological model of the Milk River Transboundary Aquifer (Alberta, Canada – Montana, USA). Can. J. Earth Sci. 52, 96–111. https://doi.org/10.1139/cjes-2014-0079

Pétré, M.-A., Rivera, A., Lefebvre, R., Hendry, M.J., Folnagy, A.J.B., 2016. A unified hydrogeological conceptual model of the Milk River transboundary aquifer, traversing Alberta (Canada) and Montana (USA). Hydrogeology Journal 24, 1847–1871. https://doi.org/10.1007/s10040-016-1433-8

Phillips, F.M., Bentley, H.W., Davis, S.N., Elmore, D., Swanick, G.B., 1986. Chlorine 36 dating of very old groundwater: 2. Milk River Aquifer, Alberta, Canada. Water Resour. Res. 22, 2003–2016. https://doi.org/10.1029/WR022i013p02003

Rabelo, J.L., Wendland, E., 2009. Assessment of groundwater recharge and water fluxes of the Guarani Aquifer System, Brazil. Hydrogeology Journal. https://doi.org/10.1007/s10040-009-0462-y

Robertson, C., 1988. Potential impact of subsurface irrigation return flow on a portion of the Milk River and Milk River Aquifer in southern Alberta. University Of Alberta Dept Of Geology.

Rivera, A., Candela, L., 2018. Fifteen-year experiences of the internationally shared aquifer resources management initiative (ISARM) of UNESCO at the global scale. Journal of Hydrology: Regional Studies. https://doi.org/10.1016/j.ejrh.2017.12.003

Schwartz, F.W., Muehlenbachs, K., Chorley, D.W., 1981. Flow-system controls of the chemical evolution of groundwater. Developments in Water Science 16, 225–243.

Swanick, G.B., 1982. The hydrochemistry and age of the water in the Milk River aquifer, Alberta, Canada. Masters thesis. The University of Arizona.

Toth, J., 1963. A theoretical analysis of groundwater flow in small drainage basins. J. Geophys. Res. 68, 4795–4812.

Toth, J., Corbet, T., 1986. Post-Paleocene evolution of regional groundwater flow-systems and their relation to petroleum accumulations, Taber area, southern Alberta, Canada. Bulletin of Canadian Petroleum Geology 34, 339–363.

Tuck, L.K., 1993. Reconnaissance of geology and water resources along the north flank of the Sweet Grass Hills, north-central Montana. U.S. Geological Survey. Water-Resources Investigations Report 93-4026. 68 p. (No. WRI-93-4026).

TWAP, 2012. Transboundary Waters Assessment Programme [WWW Document]. URL https://isarm.org/twap/twap-groundwater (accessed 10.30.18).

Voss, C.., Soliman, S.M., 2014. The transboundary non-renewable Nubian Aquifer System of Chad, Egypt, Libya and Sudan: classical groundwater questions and parsimonious hydrogeologic analysis and modeling. Hydrogeology Journal 22, 441–468. https://doi.org/10.1007/s10040-013-1039-3.

Zhou, Y., Li, W., 2011. A review of regional groundwater flow modeling. Geoscience Frontiers 2, 205–214. https://doi.org/10.1016/j.gsf.2011.03.003

Zimmerman, E., 1967. Water resources of the Cut Bank area, Glacier and Toole Counties, Montana. Montana Bureau of Mines and Geology. Bulletin 60. 37 p (No. Bulletin 60).

8. Electronic supplement material

ESM1. Hydraulic conductivity map of the MRA

The K map of the MRA (Figure 10) shows a wide range of K values from $8x10^{-9}$ to $9x10^{-4}$ m/s with higher values concentrated in the middle of the domain. This distribution is associated with faulting and fracturing around the igneous intrusion of the Sweet Grass Hills as well as structural deformation in the south-west corner of the study area (Tuck, 1993; Zimmerman, 1967).

ESM2. Model calibration levels map

To better visualize the spatial distribution of errors, the level of calibration was calculated for each calibration target. The highest degree of calibration (level 1) indicates that the simulated heads fall within the calibration target (+/- 30 m). Levels 2 and 3 correspond respectively to simulated values that fall within two and three times the associated error of the calibration target (i.e +/- 60 and 90 m) (Anderson and Woessner 1992). Table 9 shows the levels of calibration in each calibration zone of the model and the spatial distribution of the levels of calibration for each observation point is shown in Fig. 11. In southern Alberta, the calibration targets derived from the potentiometric surface of Toth and Corbet (1986) show the highest calibration level The lower levels of calibration in Montana can be explained by the uncertainties of the underlying geological model in this area. Indeed, the geological data are scarce in Montana and the resulting error in the geometry of the hydrostratigraphic units can lead to a decrease in the representative nature of the model and thus of its calibration performance. Besides, the south-east area in Montana has the largest uncertainties associated with water level observation points. These observation points are derived from a potentiometric map drawn at the regional scale that includes only a few isolines in south-east Montana (Levings 1982). The uncertainty is then higher in south-east Montana, whereas observation points derived from small scale potentiometric maps such as Tuck (1993) in the Sweetgrass Hils area or Zimmerman (1967) in the south-west Montana are more accurate. The lowest level of calibration (level 3) is found on the flanks of the eastern butte of the Sweetgrass Hills. The steep topography in this area explains the difficulty in obtaining a satisfying calibration.

Table 9 Levels of calibration for the simulated heads in the Milk River Aquifer

		Levels of calibration					
		Level 1		Level 2		Level 3	
Calibration zones	Total number of observation points	Number of obs. points	%	Number of obs. points	%	Number of obs. points	%
Montana, south-west	38	33	86.8	5	13.2	0	0.0
Montana, south-east	72	46	63.9	23	31.9	3	4.2
Montana, Sweetgrass Hills area	22	19	86.4	3	13.6	0	0.0
Alberta, south of the Milk River (Toth and Corbet 1986)	80	73	91.2	7	8.8	0	0.0
Alberta, south of the Milk River (Meyboom 1960)	80	56	70	24	30	0	0.0

ESM3. Simulated heads contour map

The calibration performance was also qualitatively assessed with the comparison of contour maps between observed and simulated heads, as shown in Fig. 12. This map shows that the regional groundwater flow patterns simulated and observed are similar in northern Montana and south of the Milk River in southern Alberta. More specifically, the groundwater divide north of Cut Bank, Montana, is well reproduced by the model. The radial pattern from the Sweetgrass Hills area to the north, east and south-east is satisfactorily replicated. In Alberta, the observed contour map is from Toth and Corbet (1986), as their interpretation of the heads distribution is in closer agreement with simulated heads.

ESM4. Simulated artesian conditions

Insert Figure 13 here

ESM5. Parameter sensitivity analysis

A sensitivity analysis was carried out to test the effect of change in parameters in achieving the calibration result on the RMSE and on the number of calibration targets with a level 1. The sensitivity of the calibration is tested by changing several parameters (one at a time) from the reference case (the calibrated model without pumping). The RMSE and the percentage of level 1 calibration targets were calculated for each simulation. The magnitude of change in RMSE and level 1 calibration target is a measure of the sensitivity of the solution to that particular parameter.

Fig. 14 shows the effect of change in the recharge rate (a), the vertical anisotropy of the Belly River (b) and Pakowki formations (c), the hydraulic conductivity of the Pakowki Formation (d), the bedrock valleys (e) and the Milk River Formation in the south-east corner of the study area (f) on the RMSE and the number of level 1 calibration targets.

Recharge rates were modified in both the outcrop area of the MRA and the remaining of the domain The recharge rate in the aquitard outcrop area remains unchanged (0 mm/y). Results are shown for the different calibration zones to illustrate areas of the model domain that are most sensitive to variations of a specific parameter.

The calibration zones in south–west Montana and in the Sweet Grass Hills are the least sensitive to tested parameters, whereas the south-east Montana and the area south of the Milk River in Alberta are the most sensitive.

In the calibration process, a compromise was reached between the minimization of the RMSE and the maximisation of the number of flowing artesian nodes north of the study area. Therefore, the calibrated value does not always minimize the RMSE in the model, rather it reflects the adjustment between a satisfying representation of the artesian conditions and the minimisation of the RMSE. For example, a recharge rate increased by a factor of 2 or 4 will increase both the artesianism and the RMSE. Therefore, the number of level 1 calibration targets is lowered in all calibration zones except in south-west Montana. When the recharge rate is lowered by a factor 2 the RMSE slightly decreases whereas the decrease in artesianism is significant (more than 10%).

The same objective was followed when testing the vertical anisotropy of the Pakowki/Claggett and Belly/Judith River formations. The area south of the Milk River in Alberta and the area in south-east Montana are the most sensitive to the change in the vertical anisotropy.

The change in artesianism is especially significant (between 8 and 10%) when varying the hydraulic conductivity of the bedrock valleys and the vertical anisotropy of the Belly/Judith River Formation. When the hydraulic conductivity of the bedrock valleys is higher than the calibrated value, the flowing artesianism tends to disappear and the buried valleys do not function as drains anymore. The vertical flux between the buried valleys and the MRA is even reversed (directed downward from the buried valleys).

The performance of the model is sensitive to the change in the hydraulic conductivity of the Pakowki Formation in south-east Montana and southern Alberta only. This result was expected as the Pakowki Formation is little or not present at all in the other calibration areas of the model.

Changing the hydraulic conductivity of the Milk River Formation in the south-east corner of the study area in Montana only affects the performance of the model in that specific area.

ESM6. Particle tracking

Insert Figure 15 here

Fig. 1. Study area and limits of the numerical groundwater flow model (continuous black line)

Fig. 2. Conceptual hydrogeological model of the MRA. Location of the cross-section AA' is shown on Fig. 1. (modified from Pétré et al. 2016)

Fig. 3. MRA 3D numerical model with geological units. Vertical exaggeration is 30 times.

Fig. 4. Boundary conditions in the model domain (h is hydraulic head and z is elevation relative to sea level): (a) specified head at the surface of the model (top of layer 1); (b) specified head at the perimeter of the Bow Island sandstone (layer 14); (c) zones of specified recharge in the MRA outcrop/subcrop area (10 mm/y) and elsewhere over the model surface (1 mm/y), except where the Colorado Group aquitard outcrops (0 mm/y); (d) summary of the boundary conditions imposed in the model.

Fig10. Hydraulic conductivity of the Milk River Aquifer (derived from Pétré et al. 2016)

Fig. 5. Delineation of the six MRA exploitation zones, along with the location of the water wells completed within the MRA and the extent of the subdomain budget (blue line).

Fig. 6. Location of the MRA water-level observation points in the model domain. A distinction is made between the observation points derived from historical potentiometric maps (squares) and those corresponding to monitoring wells (triangles). Recent pressure measurements are indicated (diamonds). Prior to MRA exploitation, flowing artesian conditions were found east and north of the line defined by Dowling (1917).

Fig. 7. Simulated versus measured heads in the Milk River aquifer (a) for the calibration zones (Fig. 6). The calibration target interval (+/- 30 m) is also shown (grey dashed lines). The calibration targets derived from monitoring wells are indicated as "data" in the legend. The measured heads in southern Alberta are from Toth and Corbet's (1986) interpretation. b Simulated heads comparison between the two interpretations of the 1960 potentiometric surface in Alberta (Toth and Corbet, 1986 and Meyboom, 1960) in the calibration zone located south of the Milk River in Alberta

ACCEPTED MANUSCRIPT

Fig. 13. Artesian conditions in the Milk River Formation (simulated natural conditions without exploitation)

Fig. 8. Simulated drawdown (m) in the MRA caused by the three exploitation scenarios (Table 1): (a) Scenario 1 (mean extraction); (b) scenario 2 (maximum extraction); (c) scenario 3 (ultimate extraction) and (d) approximate water level change (AGRA Earth and Environmental Limited, 1998) derived from observed water levels from late 1950s to late 1980s-1990s.

Fig. 9. Comparison of groundwater budget components: (a) between the conceptual model (Pétré et al. 2016) and the numerical model (simulated natural conditions); (b) between several groundwater use scenarios in the area north of the Milk River. Positive figures are inflow to the domain whereas negative values are outflow (loss from the budget domain).

Fig. 15. Particle tracking from and to the central nodes of the MRA and artesianism in the MRA (a) natural conditions; (b) mean extraction (scenario 1); (c) maximum extraction (scenario 2) and (d) ultimate extraction (scenario 3). Location of the cross section B-B' is indicated on Fig. 1

Fig. 11. Spatial distribution of hydraulic head calibration levels for the available observation points in the MRA

Fig. 12. Comparison of observed and simulated potentiometric surfaces.

Fig. 14. Parameter sensitivity analysis of the RMSE and calibration level 1 (for each calibration zone) to the following parameters: (a) Recharge rate; (b) Anisotropy ratio of the Belly River Formation; (c) Anisotropy ratio of the Pakowki Formation; (d) Hydraulic conductivity of the Pakowki Formation; (e) Hydraulic conductivity of the bedrock valleys; (f) Hydraulic conductivity of the MRA in the south-east corner of the study area

HIGHLIGHTS

- Goal to understand mechanisms controlling sustainability through numerical modeling
- Groundwater withdrawals lead to flow pattern changes over the entire flow system
- Loss of storage, capture and cross-formational flow compensate withdrawals
- The mean historical level of exploitation of the MRA appears sustainable

Declaration of interests

☒ The authors declare that they have no known competing financial interests or personal relationships that could have appeared to influence the work reported in this paper.

☐The authors declare the following financial interests/personal relationships which may be considered as potential competing interests:

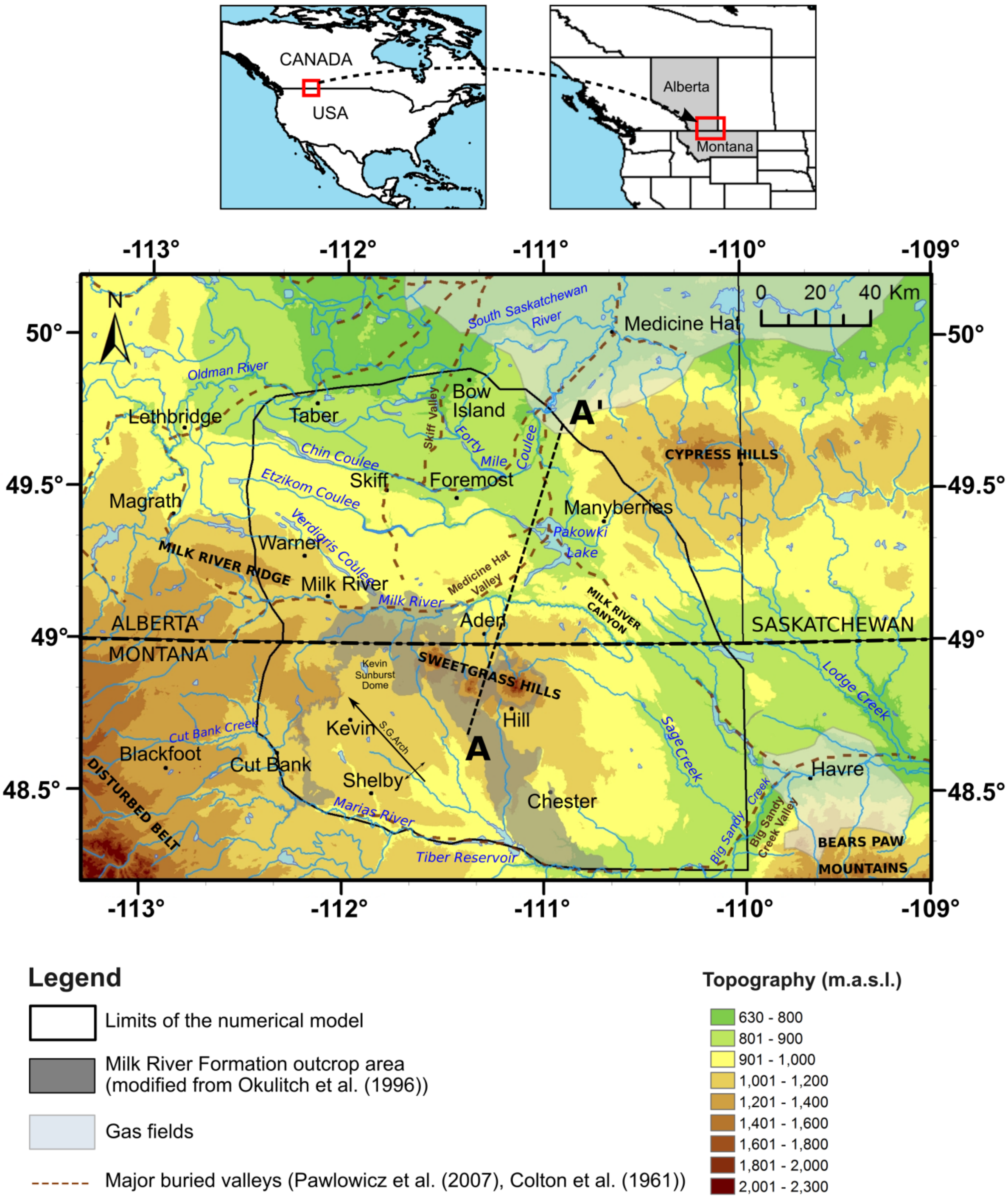
CANADA
USA
Alberta
Montana
-113°
-112°
-111°
-110°
-109°
50°
49.5°
49°
48.5°
N
0 20 40 Km
South Saskatchewan River
Medicine Hat
Oldman River
Lethbridge
Taber
Bow Island
Skiff Valley
Forty Mile Coulee
A'
CYPRESS HILLS
Chin Coulee
Skiff
Foremost
Etzikom Coulee
Magrath
Manyberries
Pakowki Lake
Verdigris Coulee
Warner
MILK RIVER RIDGE
Milk River
Medicine Hat Valley
Milk River
MILK RIVER CANYON
Aden
ALBERTA
SASKATCHEWAN
MONTANA
Kevin Sunburst Dome
SWEETGRASS HILLS
Lodge Creek
Hill
Cut Bank Creek
Kevin
S.G.Arch
A
Sage Creek
Blackfoot
Cut Bank
Havre
Shelby
DISTURBED BELT
Chester
Marias River
Big Sandy Creek
Big Sandy Creek Valley
BEARS PAW MOUNTAINS
Tiber Reservoir
Legend
Limits of the numerical model
Milk River Formation outcrop area (modified from Okulitch et al. (1996))
Gas fields
Major buried valleys (Pawlowicz et al. (2007), Colton et al. (1961))
Topography (m.a.s.l.)
630 - 800
801 - 900
901 - 1,000
1,001 - 1,200
1,201 - 1,400
1,401 - 1,600
1,601 - 1,800
1,801 - 2,000
2,001 - 2,300

1024

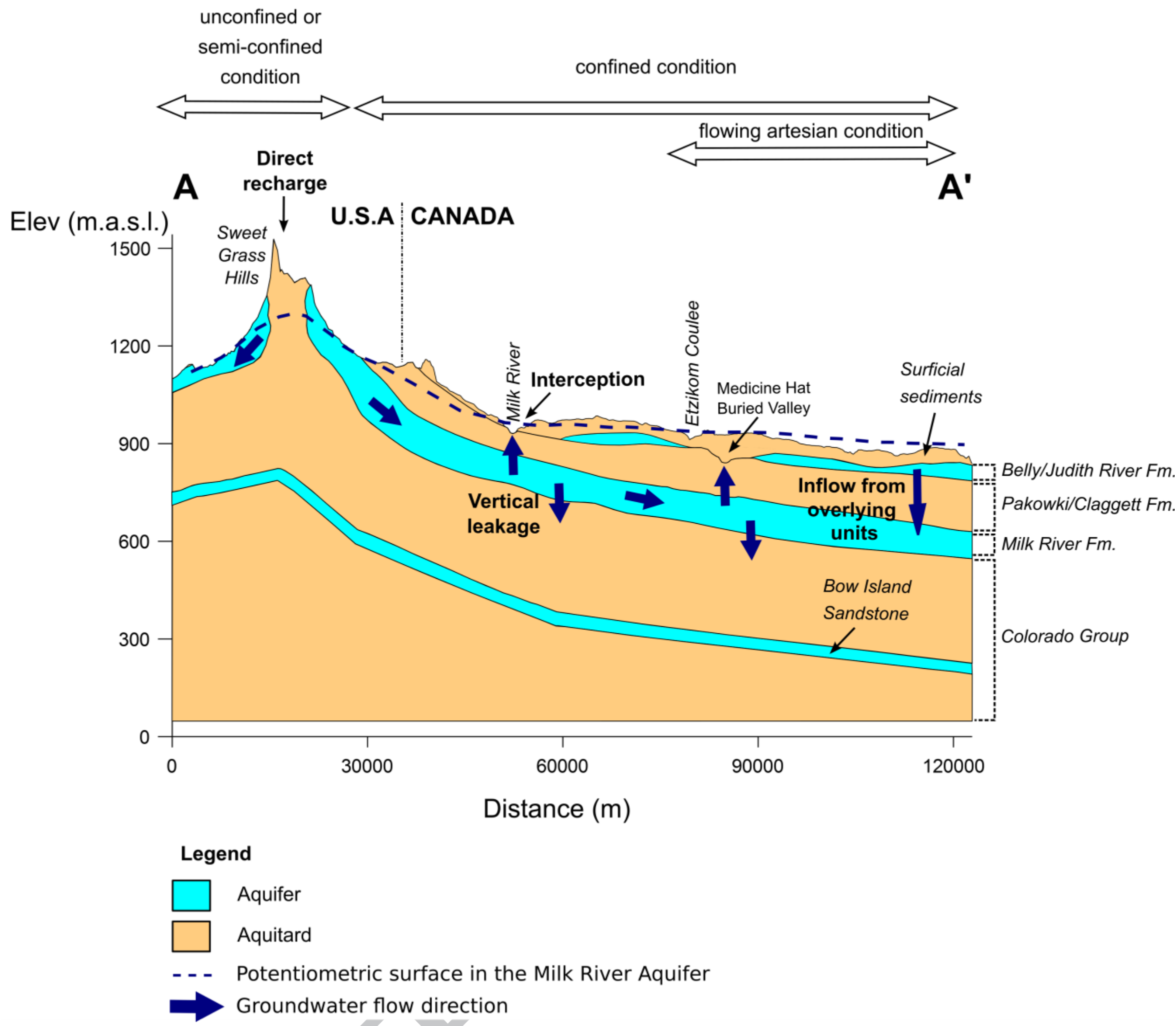
unconfined or
semi-confined
condition
confined condition
flowing artesian condition
A
Direct
recharge
A'
Elev (m.a.s.l.)
U.S.A
CANADA
Sweet
Grass
Hills
1500
1200
900
600
300
0
Milk River
Interception
Etzikom Coulee
Medicine Hat
Buried Valley
Surficial
sediments
Vertical
leakage
Inflow from
overlying
units
Belly/Judith River Fm.
Pakowki/Claggett Fm.
Milk River Fm.
Bow Island
Sandstone
Colorado Group
0
30000
60000
90000
120000
Distance (m)
Legend
Aquifer
Aquitard
Potentiometric surface in the Milk River Aquifer
Groundwater flow direction

1025

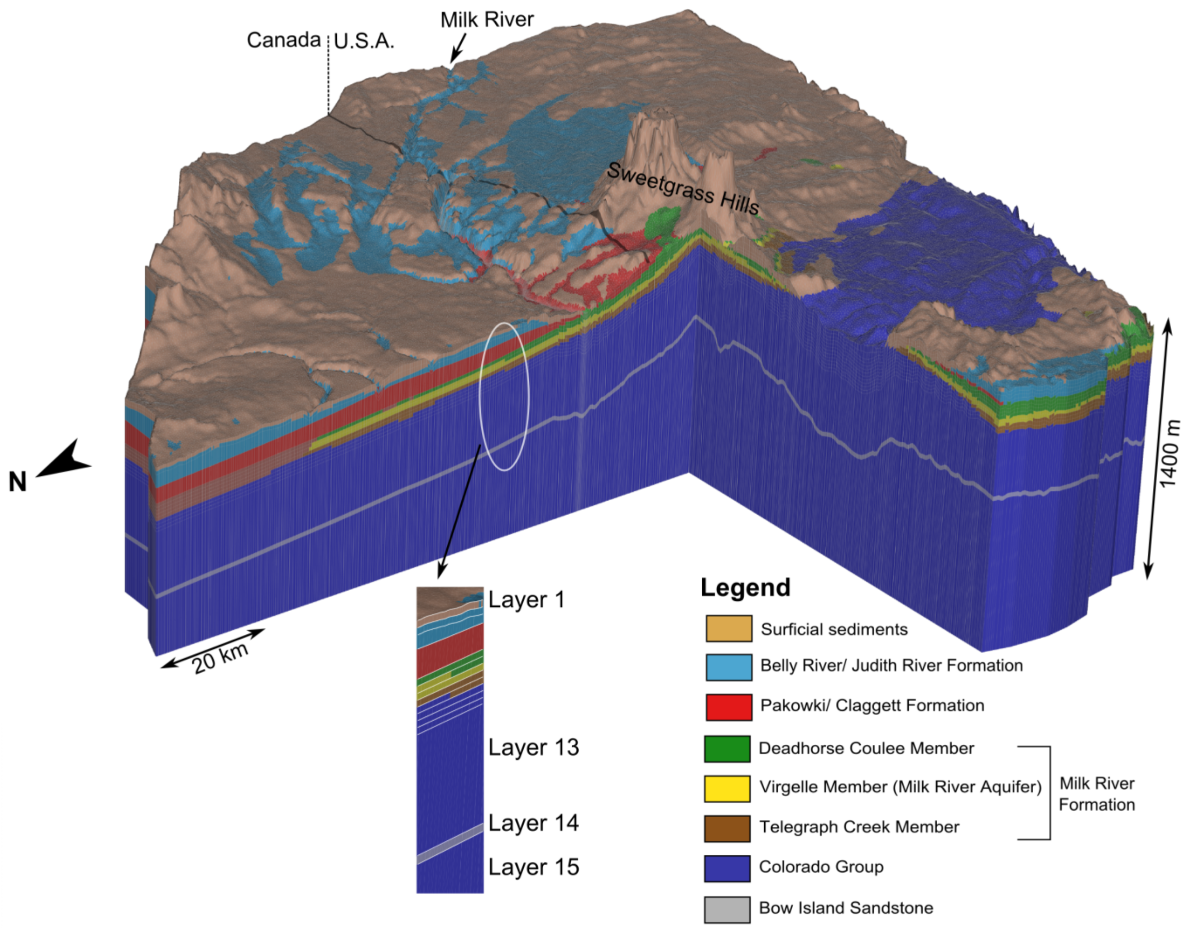
Canada
U.S.A.
Milk River
Sweetgrass Hills
N
20 km
1400 m
Layer 1
Layer 13
Layer 14
Layer 15
Legend
Surficial sediments
Belly River/ Judith River Formation
Pakowki/ Claggett Formation
Deadhorse Coulee Member
Virgelle Member (Milk River Aquifer)
Telegraph Creek Member
Milk River Formation
Colorado Group
Bow Island Sandstone

1026

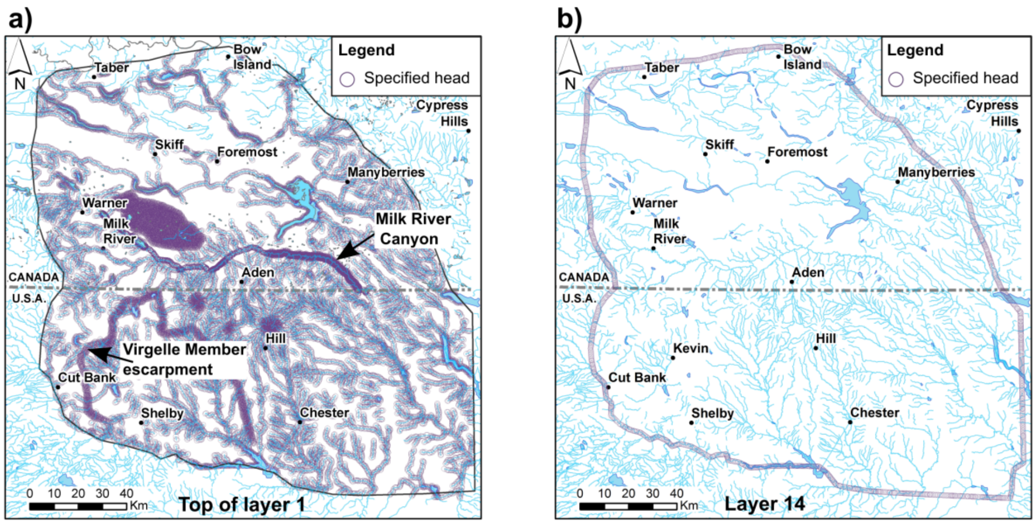

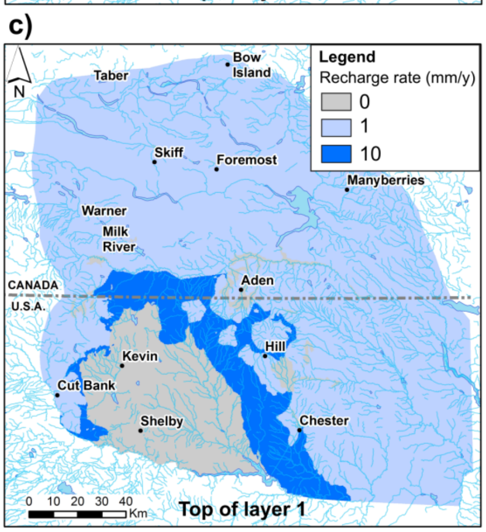

d)

Slice	Boundary type	Boundary condition
Top of layer 1 (Surface)	Specified head with seepage constraint	- Surface drainage: h=z - Virgelle member escarpment: h= z-3 m - Milk River Canyon: h= z-30 m
	Recharge	- MRA outcrop area: R= 10 mm/y - Aquitard outcrop area: R= 0 mm/y - Remaining of study area: R= 1 mm/y
Layer 14 (Bow Island Sandstone)	Specified head	- Perimeter of layer 14: h= 750 m

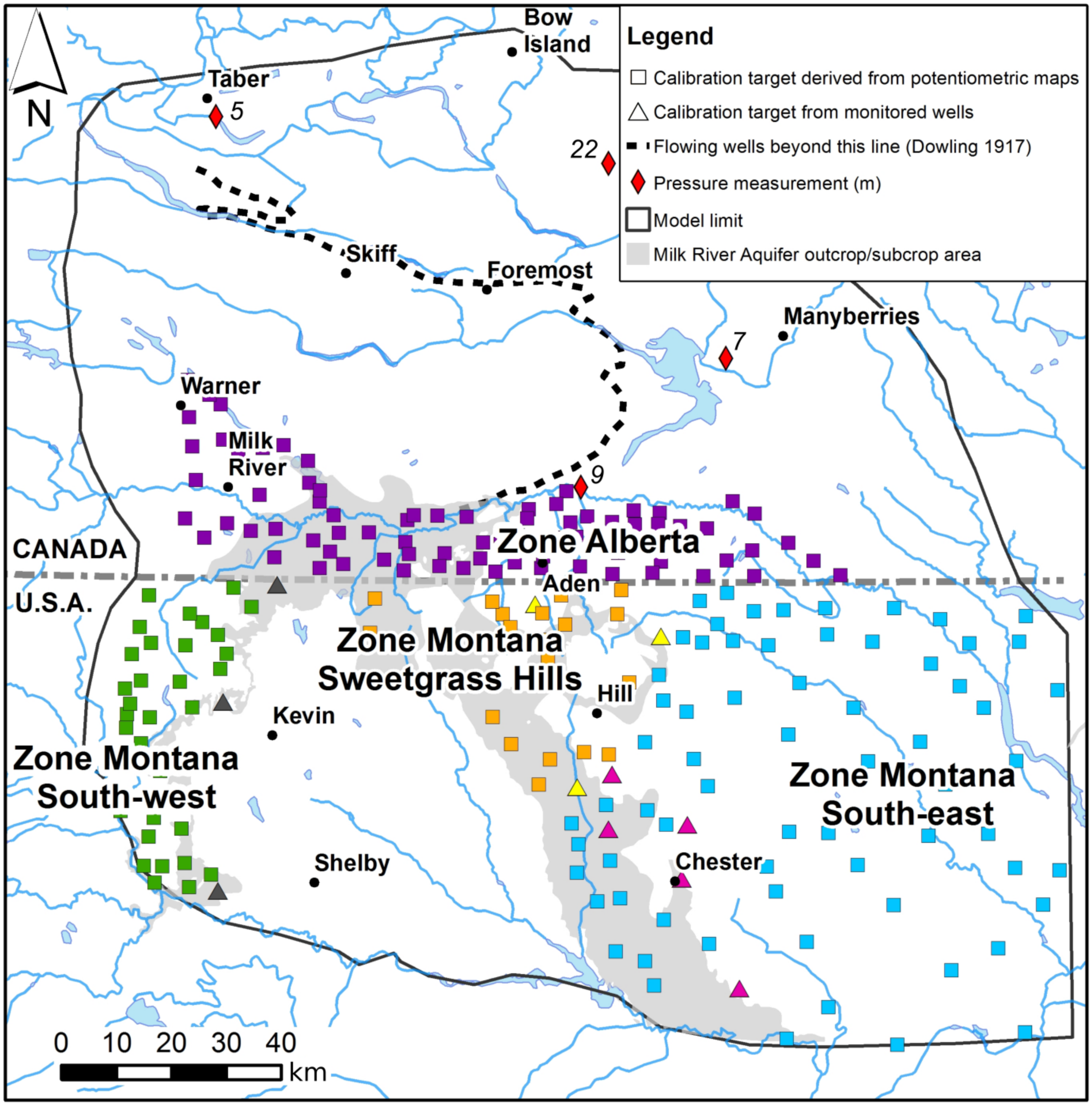

Legend
Calibration target derived from potentiometric maps
Calibration target from monitored wells
Flowing wells beyond this line (Dowling 1917)
Pressure measurement (m)
Model limit
Milk River Aquifer outcrop/subcrop area
N
Bow Island
Taber
5
22
Skiff
Foremost
Manyberries
7
Warner
Milk River
9
CANADA
U.S.A.
Zone Alberta
Aden
Zone Montana Sweetgrass Hills
Hill
Kevin
Zone Montana South-west
Zone Montana South-east
Shelby
Chester
0 10 20 30 40
km

1028

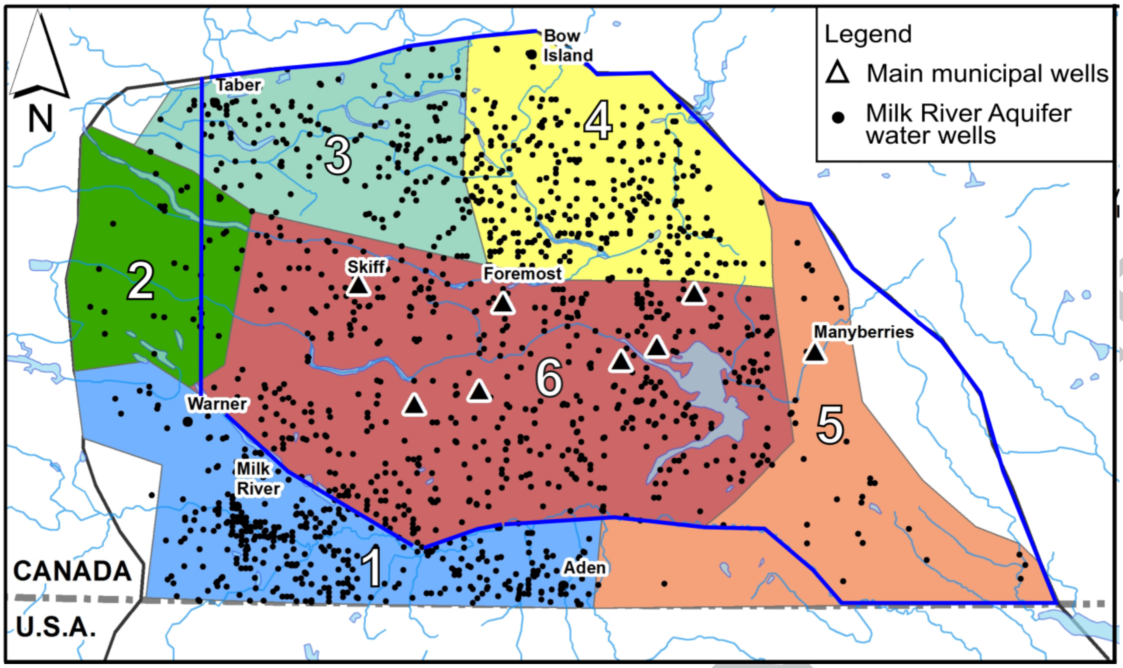
Legend
Main municipal wells
Milk River Aquifer water wells
N
Bow Island
Taber
Skiff
Foremost
Manyberries
Warner
Milk River
Aden
CANADA
U.S.A.
1
2
3
4
5
6

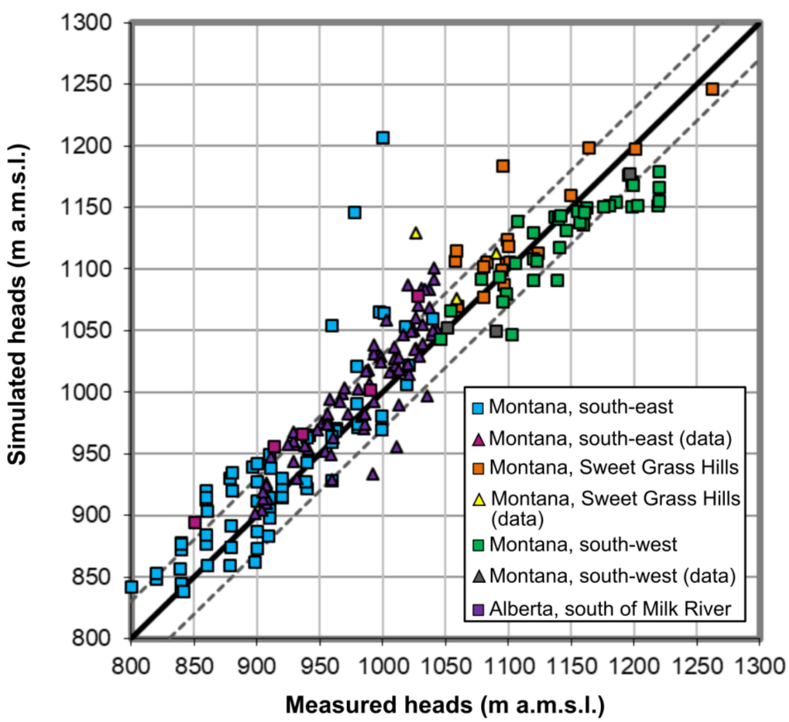
Simulated heads (m a.m.s.l.)
Measured heads (m a.m.s.l.)
Montana, south-east
Montana, south-east (data)
Montana, Sweet Grass Hills
Montana, Sweet Grass Hills (data)
Montana, south-west
Montana, south-west (data)
Alberta, south of Milk River

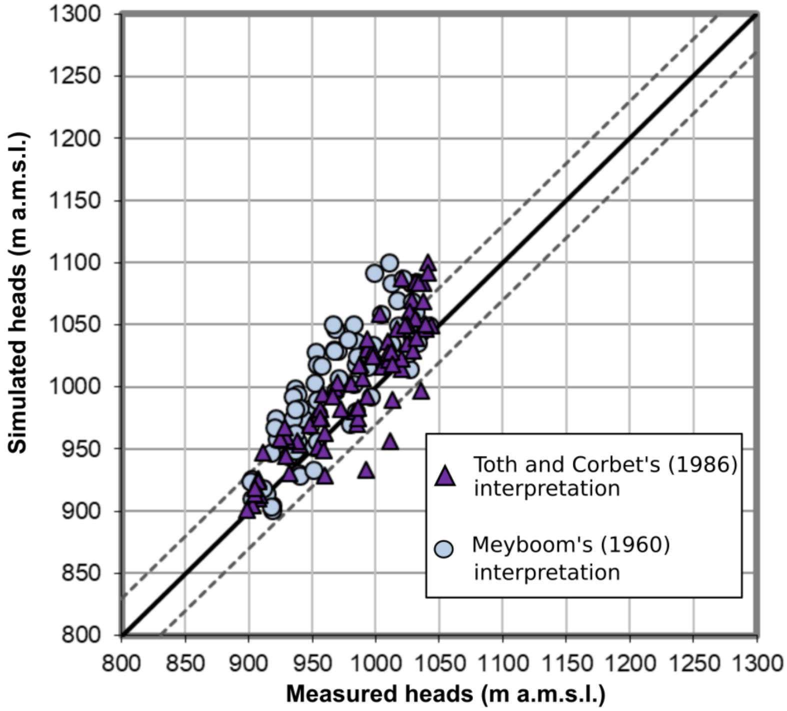

Simulated heads (m a.m.s.l.)
Measured heads (m a.m.s.l.)
800
850
900
950
1000
1050
1100
1150
1200
1250
1300
Toth and Corbet's (1986) interpretation
Meyboom's (1960) interpretation

1031

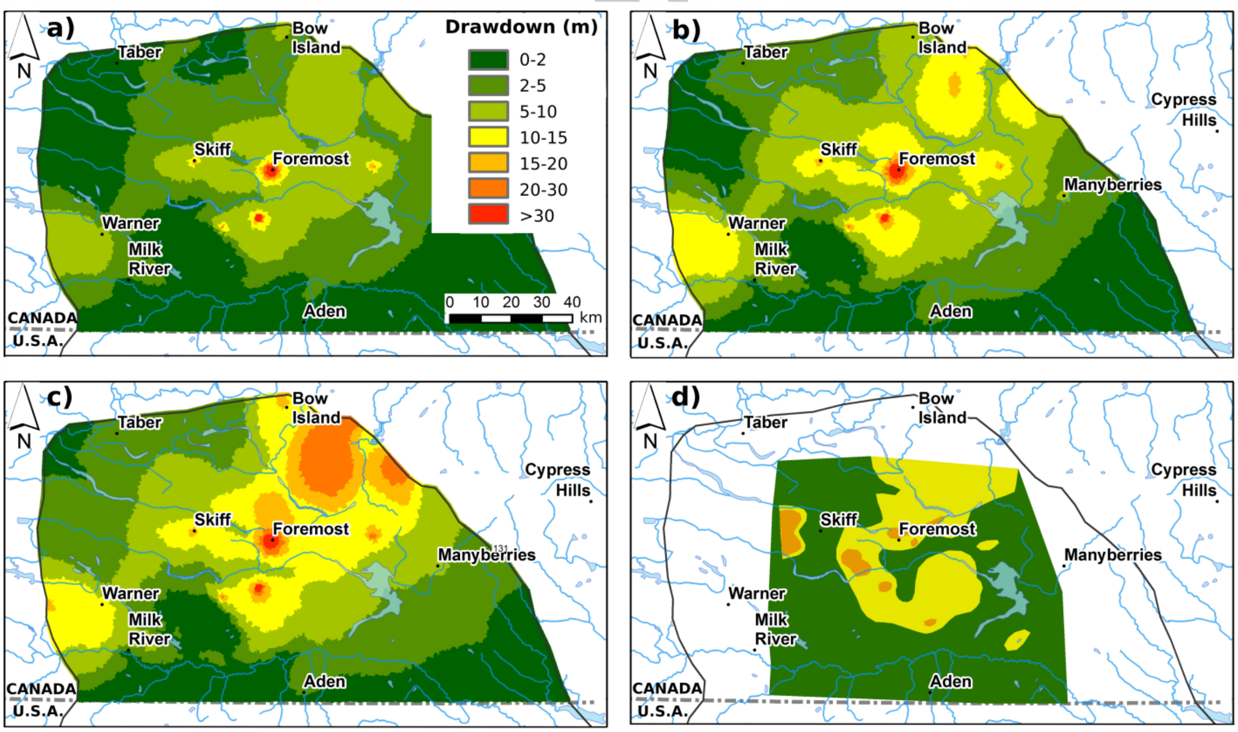

a)
b)
c)
d)
Drawdown (m)
0-2
2-5
5-10
10-15
15-20
20-30
>30
0 10 20 30 40 km
N
Bow Island
Taber
Skiff
Foremost
Warner
Milk River
Aden
Cypress Hills
Manyberries
CANADA
U.S.A.

1032

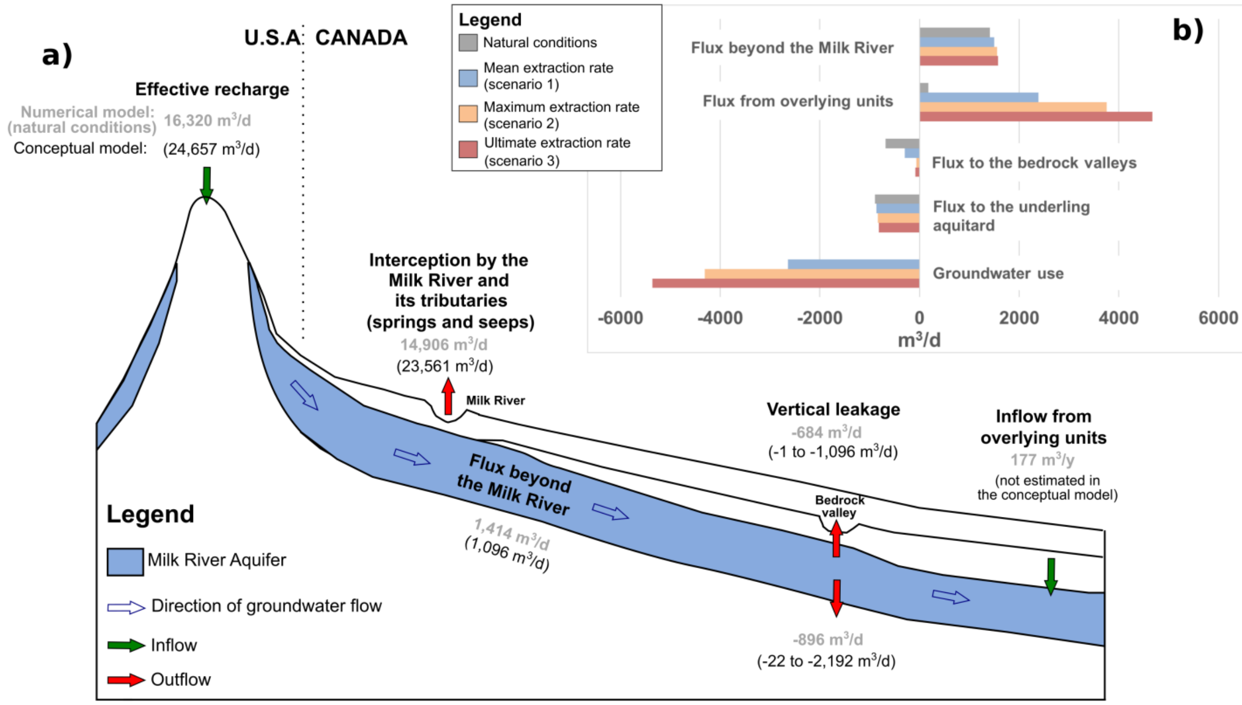
a)
U.S.A.
CANADA
Effective recharge
Numerical model: (natural conditions) 16,320 m³/d
Conceptual model: (24,657 m³/d)
Interception by the Milk River and its tributaries (springs and seeps)
14,906 m³/d
(23,561 m³/d)
Milk River
Vertical leakage
-684 m³/d
(-1 to -1,096 m³/d)
Inflow from overlying units
177 m³/y
(not estimated in the conceptual model)
Flux beyond the Milk River
1,414 m³/d
(1,096 m³/d)
Bedrock valley
-896 m³/d
(-22 to -2,192 m³/d)
Legend
Milk River Aquifer
Direction of groundwater flow
Inflow
Outflow
b)
Legend
Natural conditions
Mean extraction rate (scenario 1)
Maximum extraction rate (scenario 2)
Ultimate extraction rate (scenario 3)
Flux beyond the Milk River
Flux from overlying units
Flux to the bedrock valleys
Flux to the underling aquitard
Groundwater use
-6000
-4000
-2000
0
2000
4000
6000
m³/d

1033

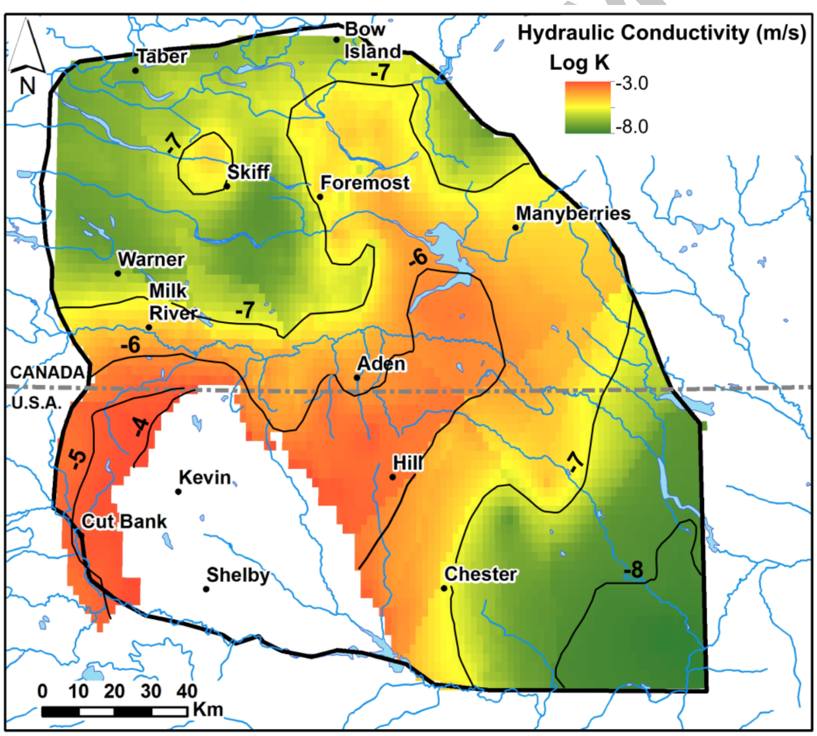
Hydraulic Conductivity (m/s)
Log K
-3.0
-8.0
N
Taber
Bow Island
Skiff
Foremost
Manyberries
Warner
Milk River
Aden
CANADA
U.S.A.
Kevin
Hill
Cut Bank
Shelby
Chester
-7
-6
-5
-4
-8
0 10 20 30 40
Km

1034

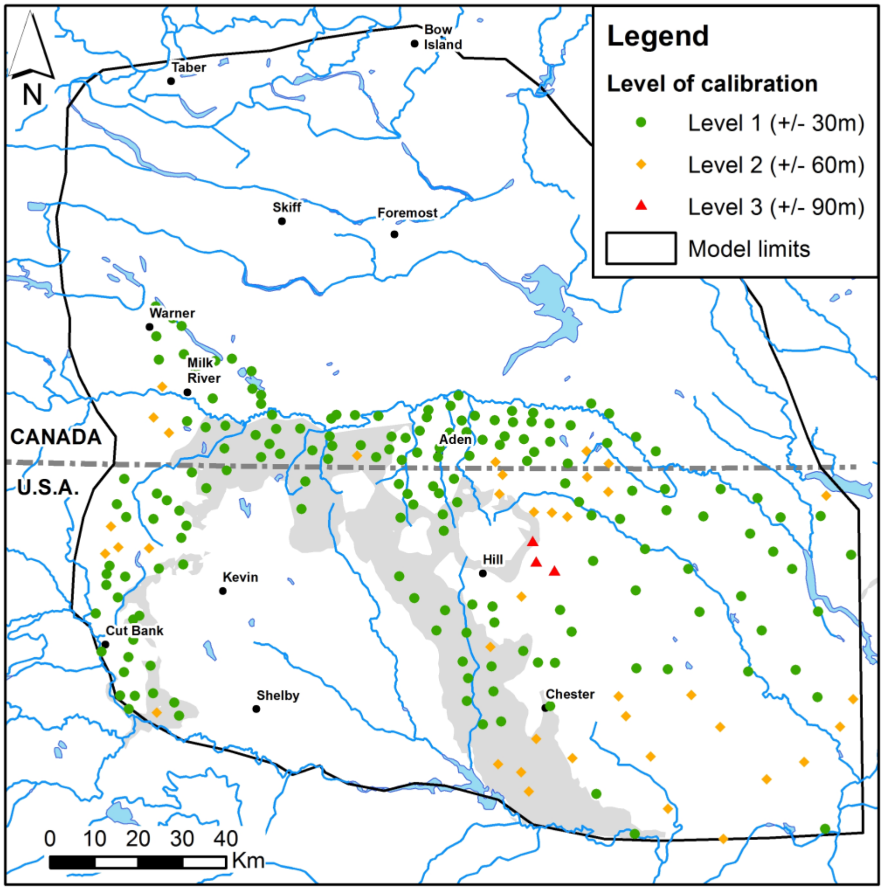

Legend
Level of calibration
Level 1 (+/- 30m)
Level 2 (+/- 60m)
Level 3 (+/- 90m)
Model limits
N
Bow Island
Taber
Skiff
Foremost
Warner
Milk River
CANADA
U.S.A.
Aden
Hill
Kevin
Cut Bank
Shelby
Chester
0 10 20 30 40
Km

1035

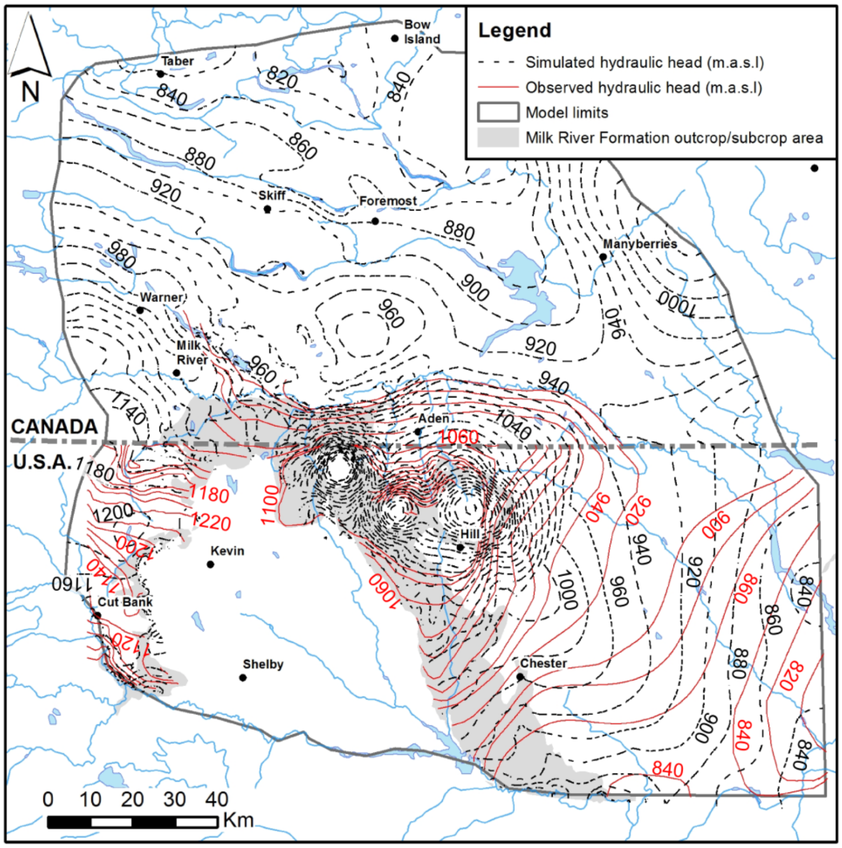
Legend
Simulated hydraulic head (m.a.s.l)
Observed hydraulic head (m.a.s.l)
Model limits
Milk River Formation outcrop/subcrop area
N
Bow Island
Taber
Skiff
Foremost
Manyberries
Warner
Milk River
Aden
CANADA
U.S.A.
Kevin
Hill
Cut Bank
Shelby
Chester
0 10 20 30 40
Km

1036

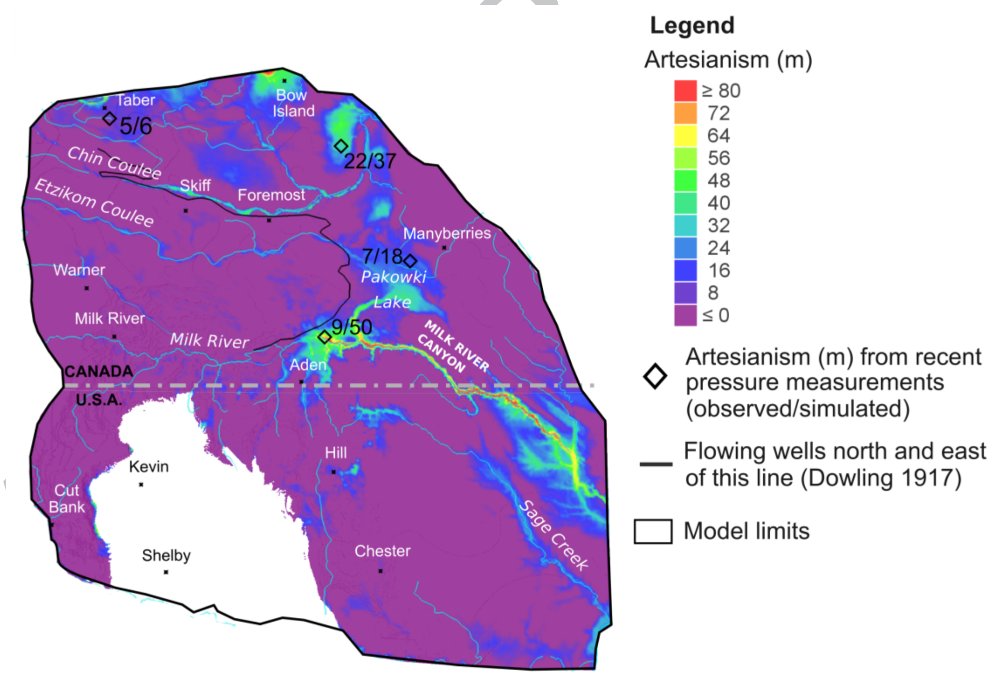
Legend
Artesianism (m)
≥ 80
72
64
56
48
40
32
24
16
8
≤ 0
Artesianism (m) from recent pressure measurements (observed/simulated)
Flowing wells north and east of this line (Dowling 1917)
Model limits
Taber
5/6
Bow Island
22/37
Chin Coulee
Etzikom Coulee
Skiff
Foremost
Manyberries
7/18
Pakowki Lake
Warner
Milk River
Milk River
9/50
MILK RIVER CANYON
Aden
CANADA
U.S.A.
Kevin
Hill
Cut Bank
Shelby
Chester
Sage Creek

1037

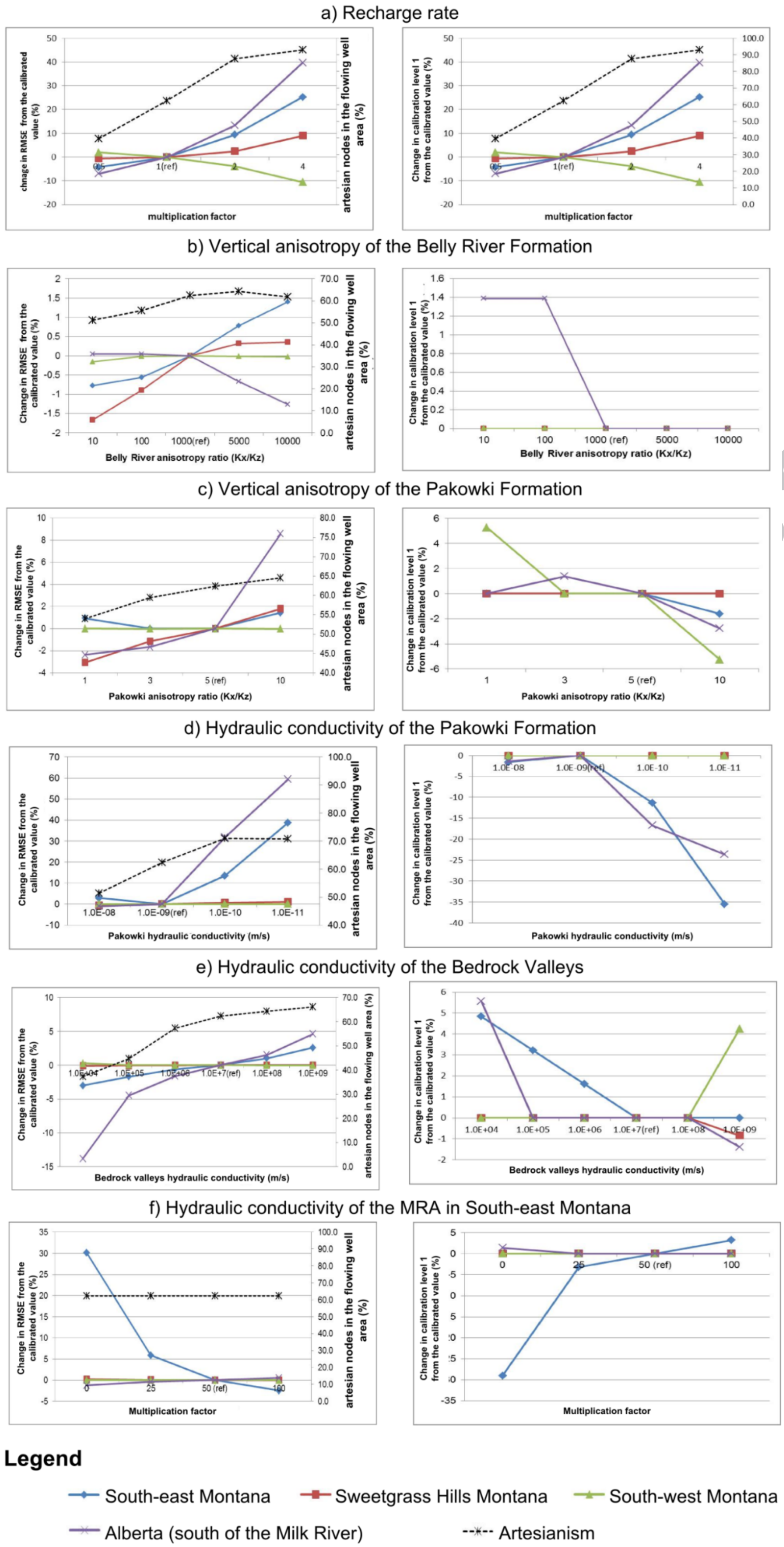
a) Recharge rate
change in RMSE from the calibrated value (%)
artesian nodes in the flowing well area (%)
multiplication factor
Change in calibration level 1 from the calibrated value (%)
b) Vertical anisotropy of the Belly River Formation
Change in RMSE from the calibrated value (%)
Belly River anisotropy ratio (Kx/Kz)
c) Vertical anisotropy of the Pakowki Formation
Change in RMSE from the calibrated value (%)
Pakowki anisotropy ratio (Kx/Kz)
d) Hydraulic conductivity of the Pakowki Formation
Pakowki hydraulic conductivity (m/s)
e) Hydraulic conductivity of the Bedrock Valleys
Bedrock valleys hydraulic conductivity (m/s)
f) Hydraulic conductivity of the MRA in South-east Montana
Multiplication factor
Legend
South-east Montana
Sweetgrass Hills Montana
South-west Montana
Alberta (south of the Milk River)
Artesianism

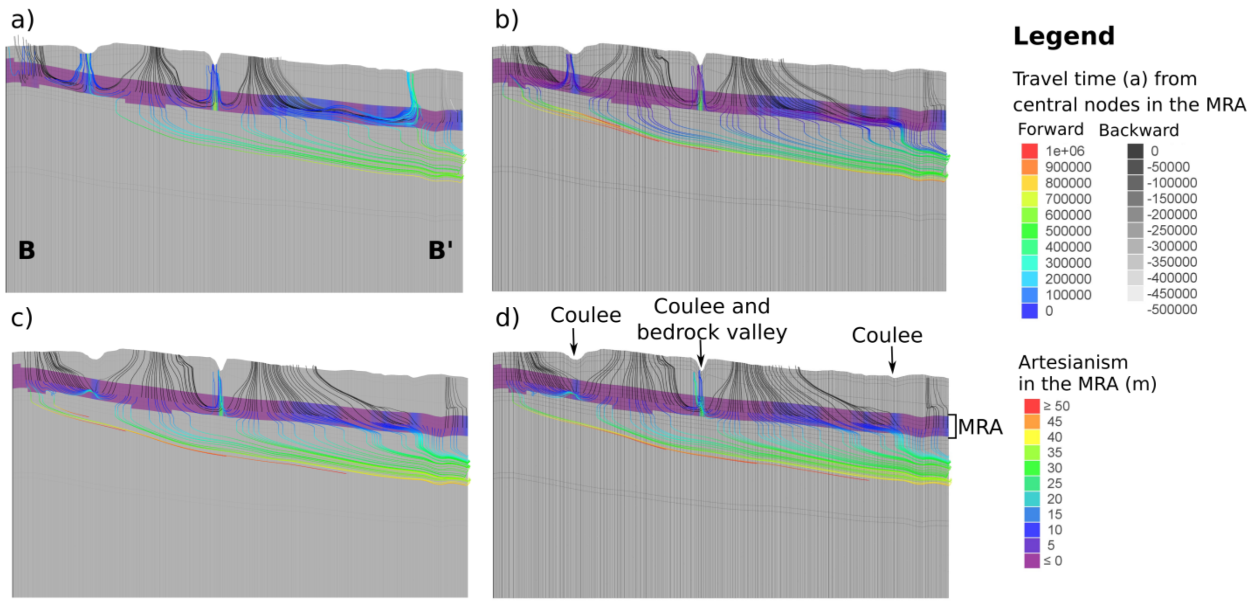

a)
b)
c)
d)
B
B'
Coulee
Coulee and bedrock valley
Coulee
MRA
Legend
Travel time (a) from central nodes in the MRA
Forward
Backward
1e+06
900000
800000
700000
600000
500000
400000
300000
200000
100000
0
0
-50000
-100000
-150000
-200000
-250000
-300000
-350000
-400000
-450000
-500000
Artesianism in the MRA (m)
≥ 50
45
40
35
30
25
20
15
10
5
≤ 0